Electronic Supplementary Material (ESI) for Journal of Materials Chemistry A.

Supporting Information

Synergic morphology engineering and pore functionality within a metal-organic framework for trace CO_2 capture

Peng Hu [a], Hao Liu [a], Hao Wang [a], Jie Zhou [a], Yongqing Wang [a,*] and Hongbing Ji [a,b,*]

[a] Fine Chemical Industry Research Institute, School of Chemistry, Sun Yat-Sen University, Guangzhou, 510275, P.R., China.

[b] School of Chemical Engineering, Guangdong University of Petrochemical Technology, Maoming, 525000, P.R. China.

[*] Corresponding author: Hongbing Ji (jihb@mail.sysu.edu.cn), Yongqing Wang (wangyq223@mail.sysu.edu.cn)

Table of Contents

1. Computational details

All the calculations including the geometry optimization and adsorption conformation, etc. were all performed in the Material Studio 7.0 package.

1.1. Periodic Density Functional Theory (PDFT) calculation

The initial structures of all the materials and guest molecules are first optimized in the Dmol^3 module, adopting the generalized gradient approximation (GGA) with the Perdew-Burke-Ernzerhof (PBE) functional. The energy, force and displacement convergence criterions were set as 1×10^{-5} Ha, 2×10^{-3} Ha and 5×10^{-3} Å, respectively. To obtain the gas binding energy, an isolated gas molecule placed in a cell unit (with the same cell dimensions as the MOF crystal). The static binding energy (at $T = 0$ K) could be expressed: $E_B = E$ (MOF) + E (gas) - E (MOF + gas) [1].

1.2. Grand Canonical Monte Carlo (GCMC) calculation

The preferential binding conformation between guests and MOF structure were initially searched through GCMC simulations. Note that host framework and the gas molecule were both rigid in GCMC simulations through using Metropolis method, so that the produced the host-guest binding energies were equal to adsorption enthalpies. For all the GCMC simulations, the frameworks and the gas molecules were described by the universal forcefield (UFF), and QEq charges were employed to the atoms of the framework and guest molecules, respectively. The loading steps, equilibration steps and the production steps were all set to 1.0×10^6 and the temperature was set at 298 K. The cut-off radius was chosen as 15.5 Å for the Lennard-Jones (LJ) potential and the long-

range electrostatic interactions were handled by the Ewald & Group summation method.

1.3. Molecular dynamics (MD) simulations

The classical molecular dynamics (MD) simulations were performed in the Forcite module. The initial configurations for the MD simulations were produced by the GCMC simulation. The framework and the gas molecule were both deemed as rigid character and the cutoff radius was chosen as 15.5 Å for the LJ potential. The constant-volume & temperature (NVT) ensemble was used to simulate the dynamic processes. The electrostatic interactions and the van der Waals interactions were evaluated by the Ewald summation method, with a Buffer width of 0.5 Å.

2. Calculation of the separation potential

2.1. Dual Langmuir-Freundlich parameter fits

Dual-Langmuir-Freundlich isotherm model was adopted to fit the single-component loadings for CO_2, N_2 and CH_4 at 298 K, as shown in Equation 1 and 2:

$$q = N_1 \frac{ap^b}{1 + ap^b} + N_2 \frac{cp^d}{1 + cp^d} \quad (1)$$

With *T*-dependent parameters *a* and *c*,

$$a = a_0 exp\left(\frac{E_A}{RT}\right); c = c_0 exp\left(\frac{E_B}{RT}\right) \quad (2)$$

The fitting parameters were listed in Table S7.

2.2. Calculations of ideal adsorbed solution theory

The gas adsorption selectivity at 298 K and 1 bar was calculated using ideal adsorbed solution theory (IAST) on the basis of the single-component adsorption data. The

adsorption selectivity for CO_2/CH_4 and CO_2/N_2 separation is defined by Equation 3:

$$S_{ads} = \frac{q_1 / q_2}{p_1 / p_2} \quad (3)$$

In above equation, the fitting parameters q_1 and q_2 reflected the molar adsorption in the adsorbed phase in equilibrium with the bulk gas phase with partial p_1 and p_2. In this work, dual-site Langmuir-Freundlich (DSLF) model was applied to fit CO_2, N_2 and CH_4 isotherms on the samples.

2.3. Calculations of isosteric heat

The isosteric heat (Q_{st}), being the crucial thermodynamic variable in adsorption process, affording serviceable information about the binding affinity between the adsorbate molecules and the adsorbent surfaces at different coverage. For this sake, the coverage-dependent adsorption enthalpy was evaluated from sorption data profiles measured at 298 and 318 K by adopting virial fitting method. In detail, a Virial-type equation mainly contained parameters a_i and b_i, which were independent of temperature. In the equation, a_i and b_i represent the fitting Virial coefficients, m and n stands for the numbers of coefficients needed to precisely the isotherms, as shown in Equation 4:

$$\ln P = \ln n + \frac{1}{T}\sum_{i=0}^{l} a_i n^i + \sum_{j=0}^{m} b_j n^j \quad (4)$$

The value of isosteric heat (Q_{st}) could be achieved by virtue of following Clausius-Clapeyron equation, as defined in Equation 5:

$$Q_{st} = -R\left[\frac{\partial \ln p}{\partial (1/T)}\right]_n = -R\sum_{i=0}^{l} a_i \qquad (5)$$

Notation

b_A	Langmuir-Freundlich constant for species i at adsorption site A, $P_a^{-\nu_{iA}}$
b_B	Langmuir-Freundlich constant for species i at adsorption site A, $P_a^{-\nu_{iB}}$
E	Energy parameter, J mol^{-1}
Q_{st}	Isosteric heat of adsorption, J mol^{-1}
c_i	molar concentration of species i in gas mixture, mol m^{-3}
c_{i0}	molar concentration of species i in gas mixture at inlet to adsorber, mol m^{-3}
t	Time, s
T	Absolute temperature, K

Greek letters

ν	Freundlich exponent, dimensionless

3. Supporting Figures

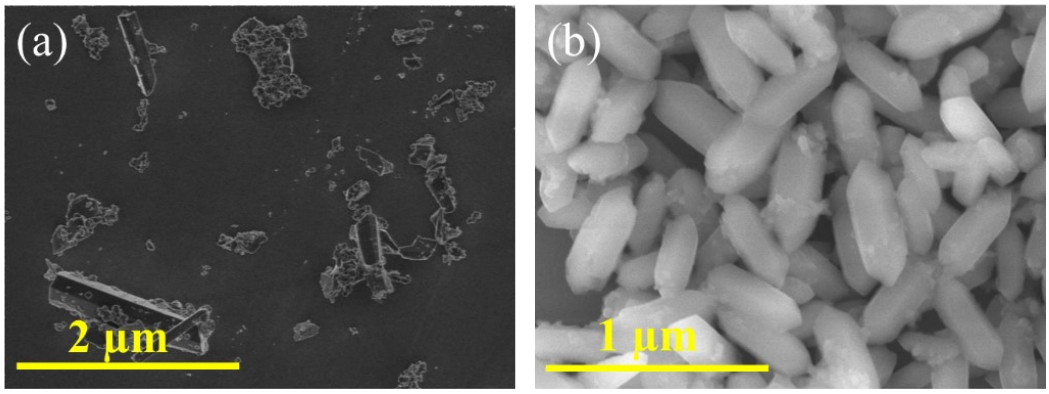

Figure S1. SEM images of (a) Co-MOF prepared by traditional solvothermal method and (b) pyz-functionalized **1a'** through facile heating procedure.

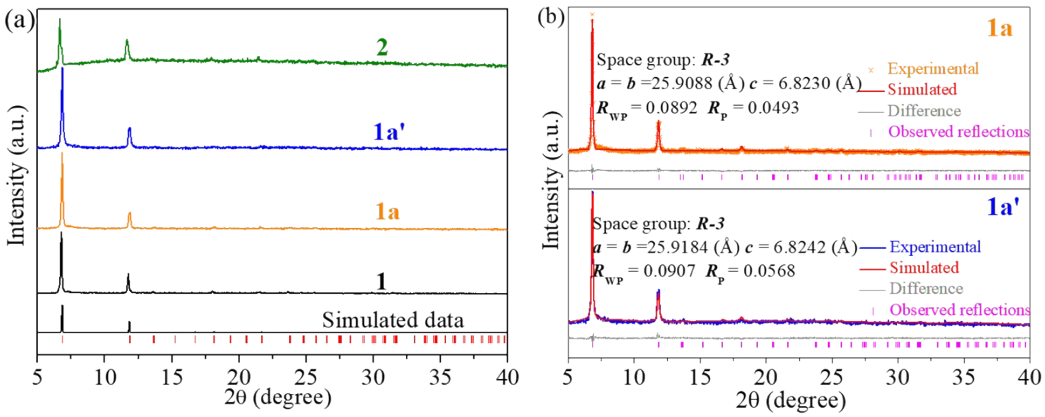

Figure S2. Powder X-ray diffraction (PXRD) of (a) as-prepared materials and (b) corresponding Rietveld structural refinements of **1a** and **1a'** using GSAS package.

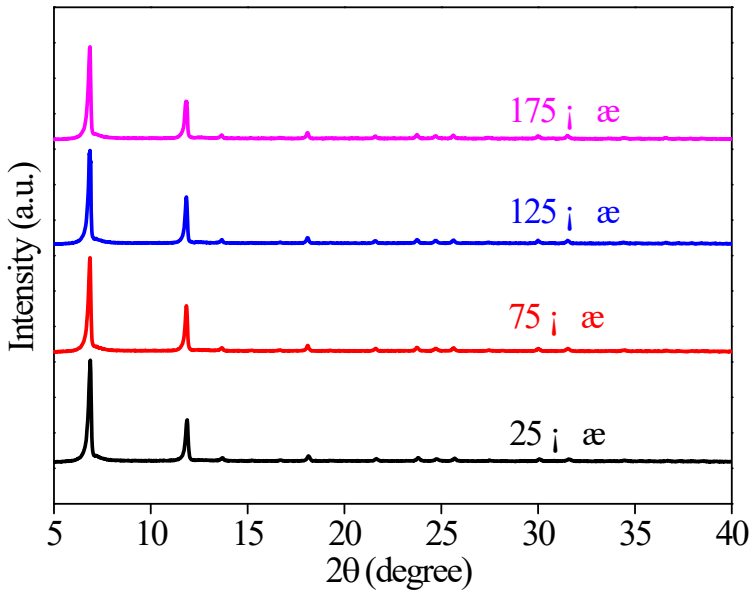

Figure S3. Experimental powder PXRD patterns for **1a'** recorded at variable temperatures.

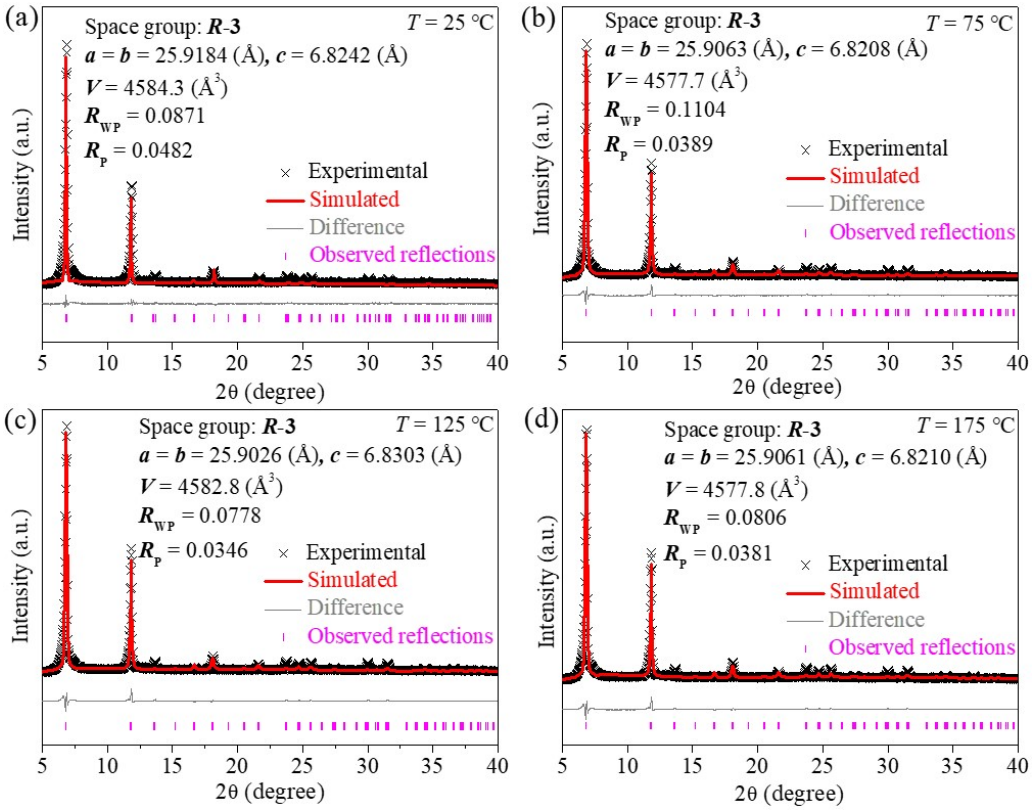

Figure S4. Rietveld structural refinements of **1a'** recorded at variable temperatures. Unit-cell parameters were obtained by using GSAS package**.**

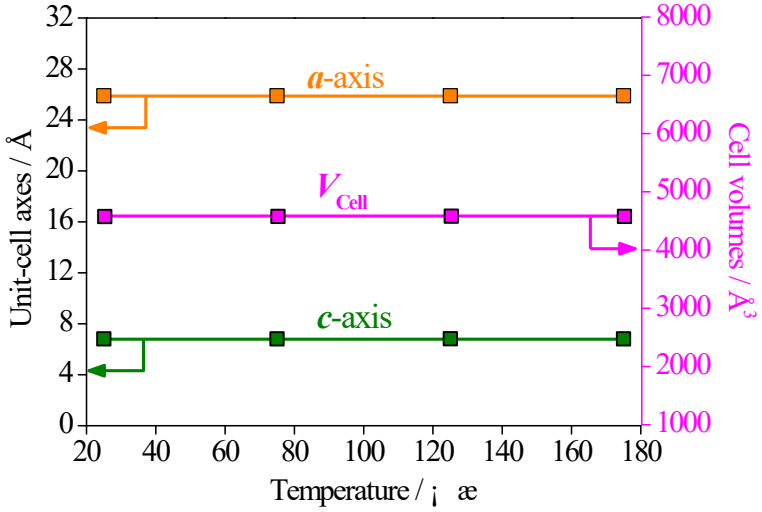

Figure S5. Variable-temperature unit-cell parameters for **1a'**.

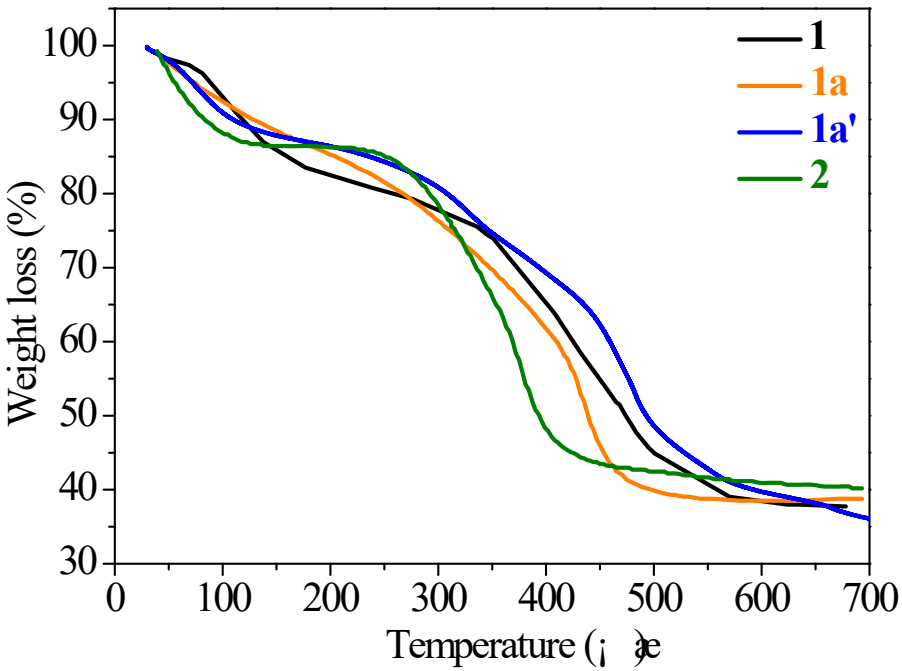

Figure S6. TGA plots for all the materials under N_2 flux with a heating rate of 5 °C per minute.

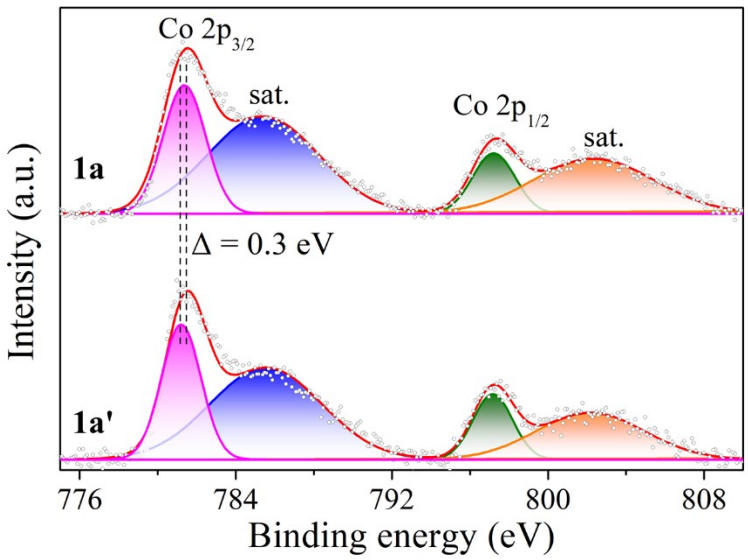

Figure S7. High resolution of Co 2p XPS in **1a** and **1a'**.

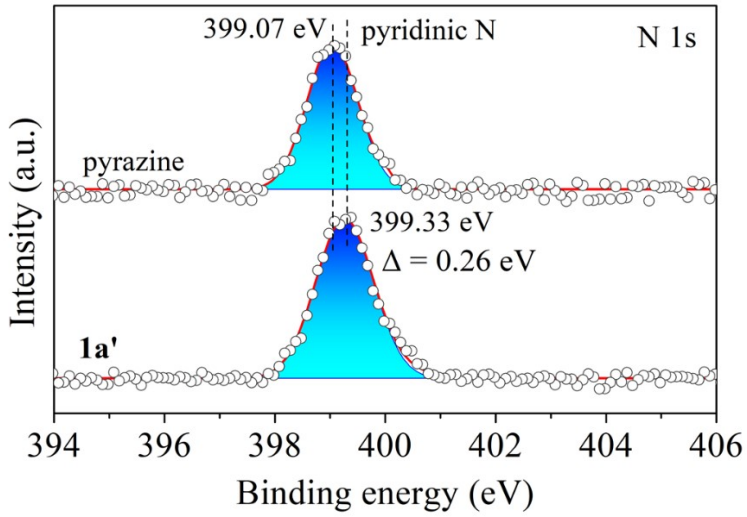

Figure S8. High resolution of N 1s XPS in pyrazine and **1a'**.

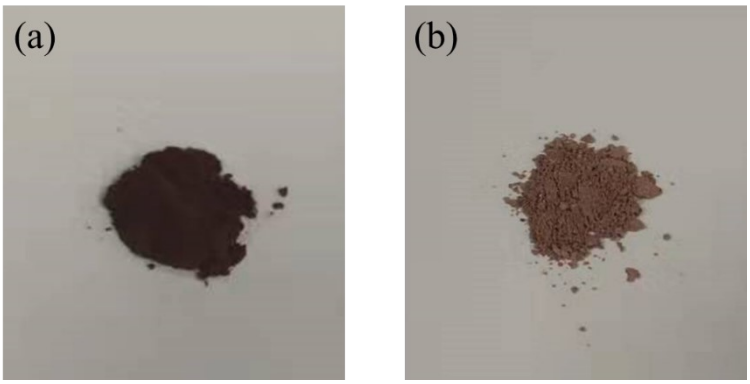

Figure S9. Photograph images of (a) **1a** and (b) **1a'** powder.

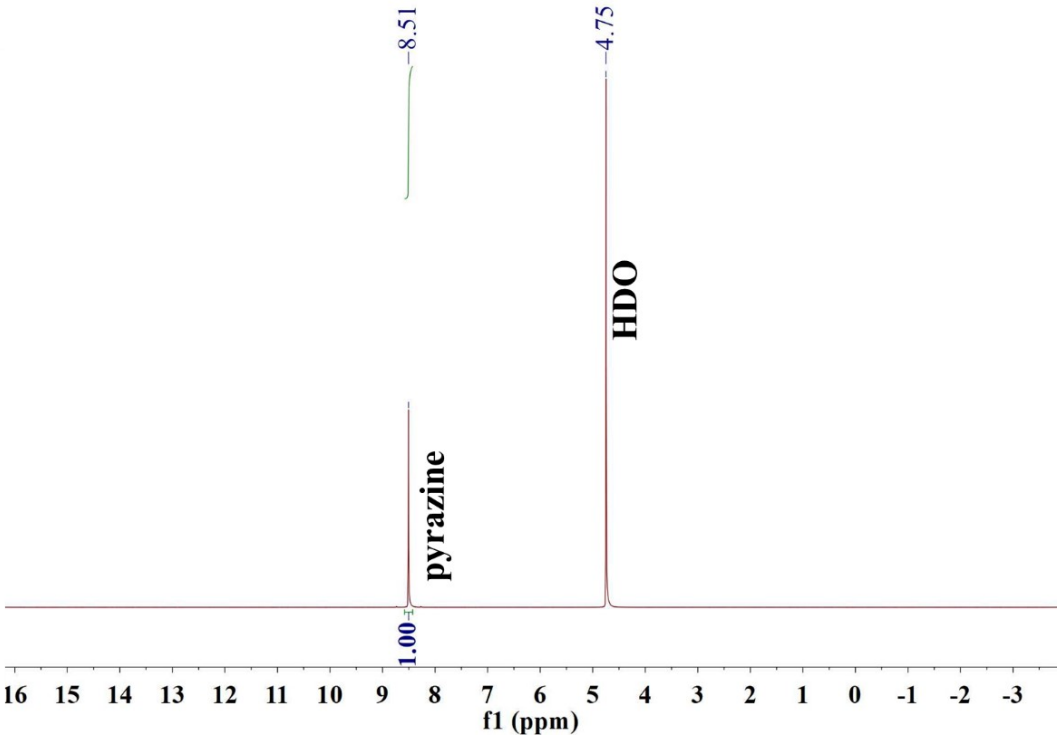

Figure S10. ^{1}H NMR spectrum of digested pyrazine (pyz) in 1 M NaOH/D_2O for 24 h.

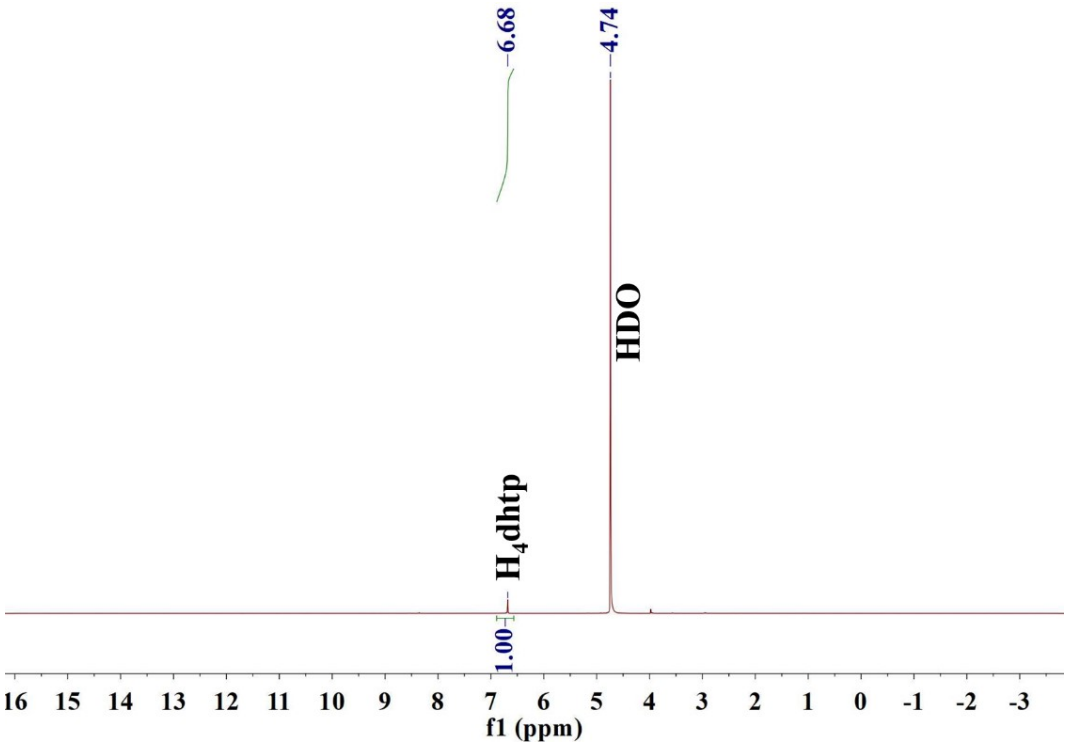

Figure S11. ^{1}H NMR spectrum of digested H_4dhtp in 1 M NaOH/D_2O for 24 h.

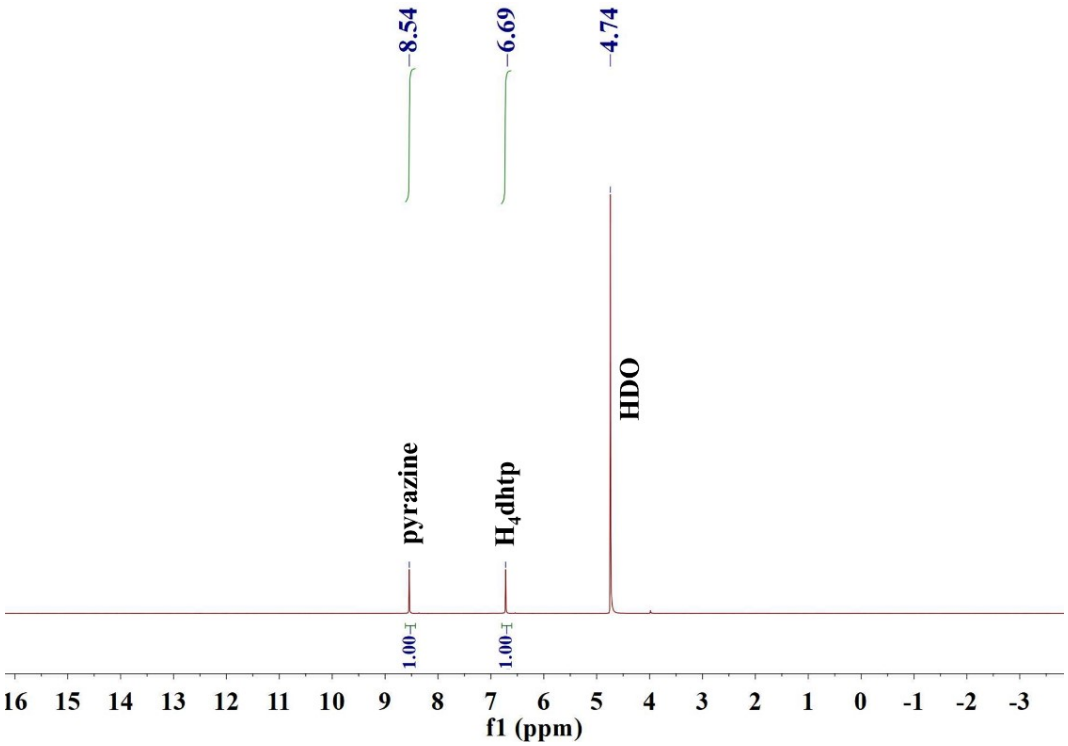

Figure S12. ^{1}H NMR spectrum of digested **1a'** in 1 M NaOH/D_2O for 24 h.

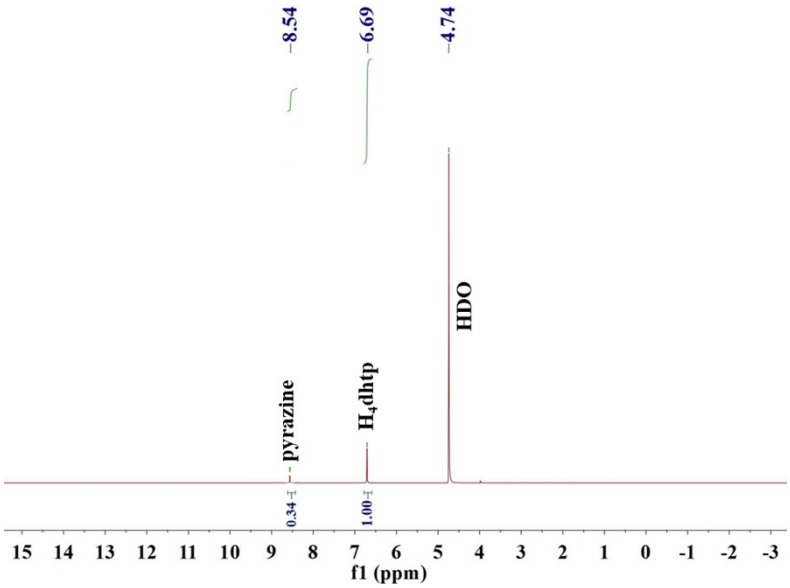

Figure S13. ^{1}H NMR spectrum of digested **2** in 1 M NaOH/D_2O for 24 h.

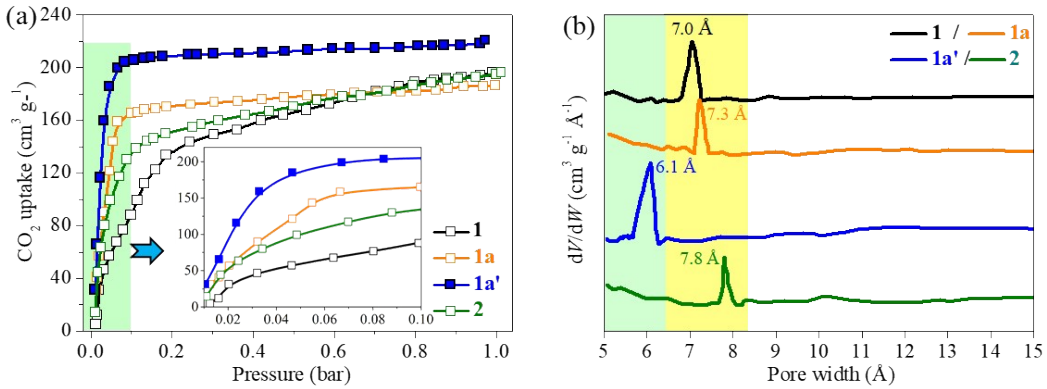

Figure S14. (a) Adsorption isotherms of CO_2 on the selected materials at 195 K and 1 bar, (b) Pore size distribution of materials using Horvath-Kawazoe model.

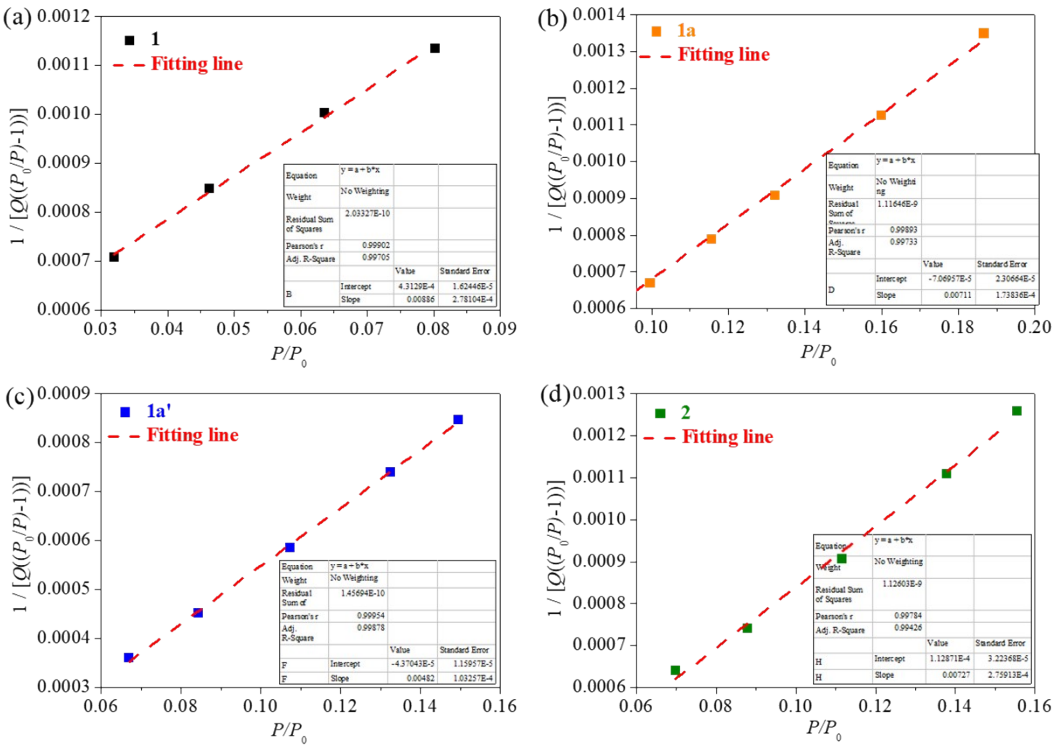

Figure S15. Plot of the linear region on the CO_2 isotherm at 195 K of materials for the BET equation.

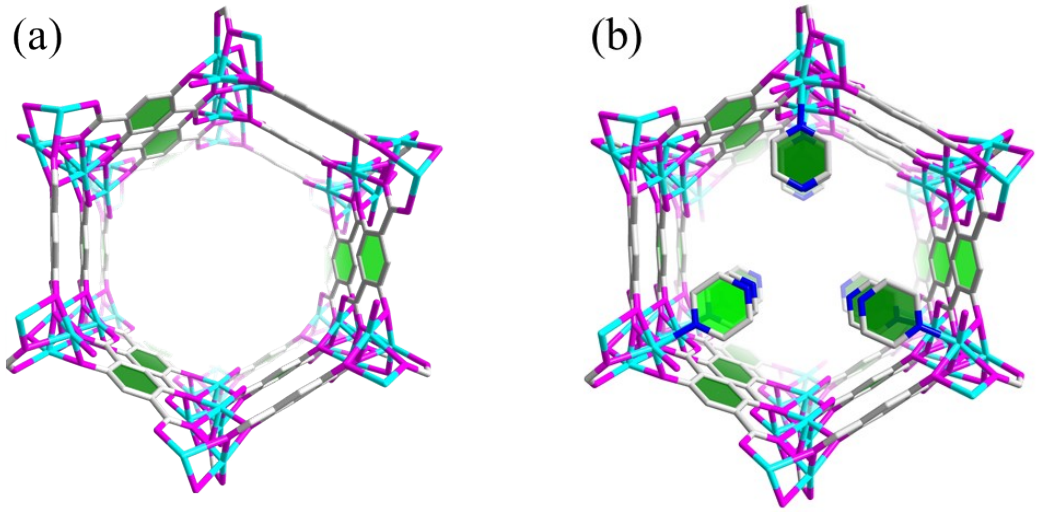

Figure S16. DFT-D optimized pore geometry in (a) **1a** and (b) **1a'**.

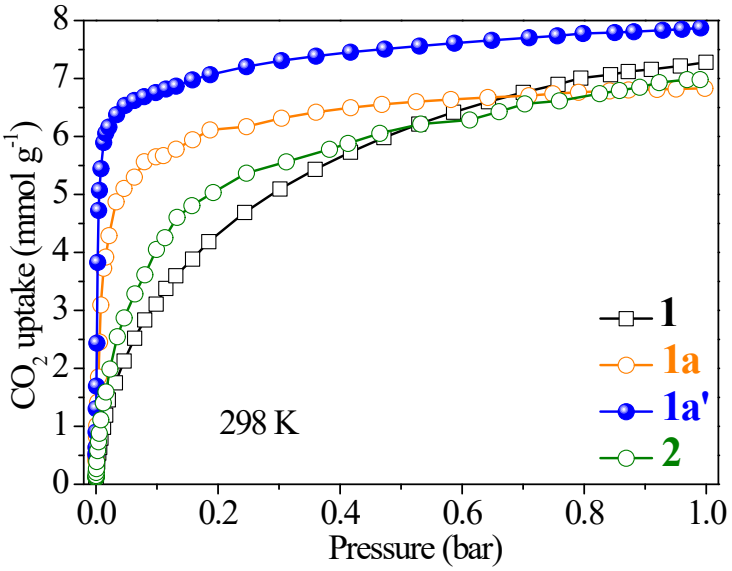

Figure S17. CO_2 adsorption isotherms of as-prepared samples measured at 298 K and 1 bar with a linear abscissa.

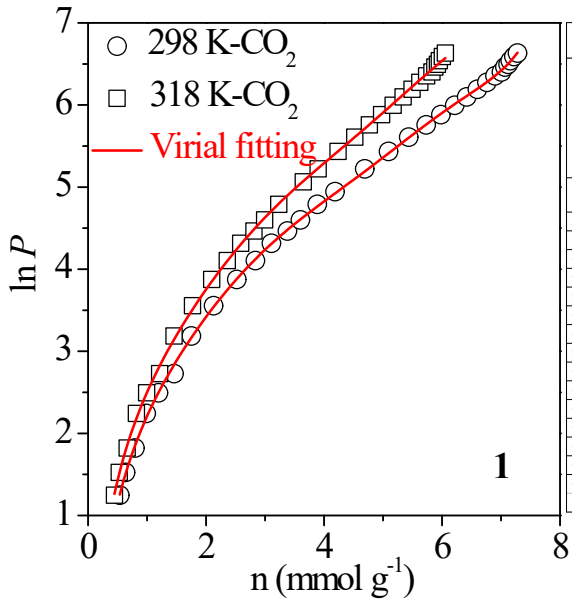

Model	Virialfitting (User)		
Equation	y = ln(x)+1/T*(a0+a1*x+a2*x^2+a3*x^3+a4*x^4+a5*x^5+a6*x^6+a7*x^7)+(b0+b1*x+b2*x^2+b3*x^3)		
Reduced Chi-Sqr			0.00101
Adj. R-Square			0.99964
		Value	Standard Error
G	T	298	0
G	a0*	-2822.01293	87.06921
G	a1*	674.00123	158.50083
G	a2*	1500.223	194.86782
G	a3*	-2414.0014	116.71153
G	a4*	143.01239	37.48539
G	a5*	4578.02923	6.61957
G	a6*	-1088.09123	0.60477
G	a7*	108.0349	0.02232
G	b0*	5.7695	0.21354
G	b1*	2.12039	0
G	b2*	0.06756	0.01077
G	b3*	0	0
I	T	318	0

Figure S18. Virial fitting (lines) of the CO_2 adsorption isotherms over **1** measured at 298 and 318 K.

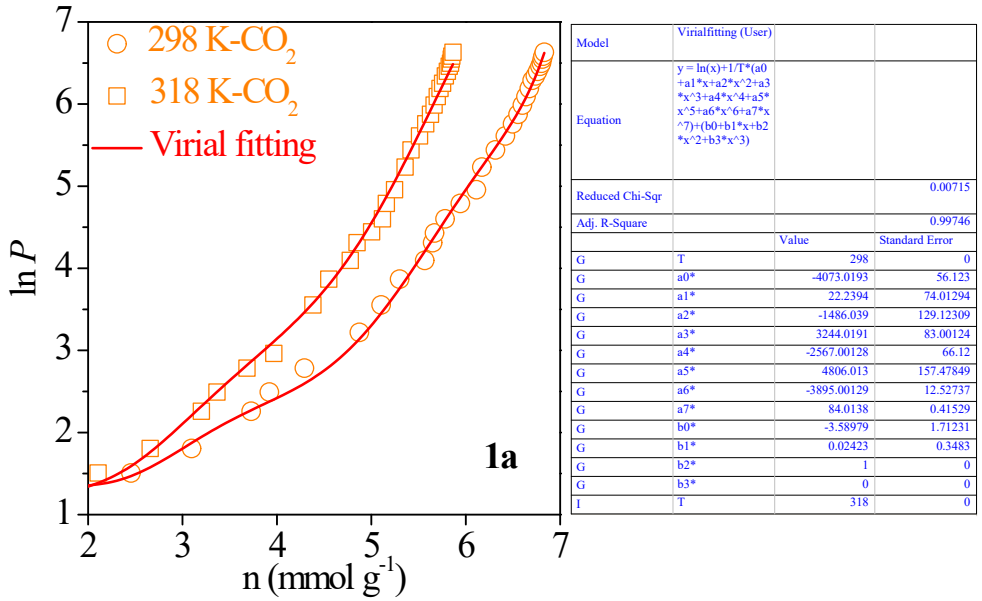

Model	Virialfitting (User)		
Equation	y = ln(x)+1/T*(a0 +a1*x+a2*x^2+a3 *x^3+a4*x^4+a5* x^5+a6*x^6+a7*x ^7)+(b0+b1*x+b2 *x^2+b3*x^3)		
Reduced Chi-Sqr			0.00715
Adj. R-Square			0.99746
		Value	Standard Error
G	T	298	0
G	a0*	-4073.0193	56.123
G	a1*	22.2394	74.01294
G	a2*	-1486.039	129.12309
G	a3*	3244.0191	83.00124
G	a4*	-2567.00128	66.12
G	a5*	4806.013	157.47849
G	a6*	-3895.00129	12.52737
G	a7*	84.0138	0.41529
G	b0*	-3.58979	1.71231
G	b1*	0.02423	0.3483
G	b2*	1	0
G	b3*	0	0
I	T	318	0

Figure 19. Virial fitting (lines) of the CO_2 adsorption isotherms over **1a** measured at 298 and 318 K.

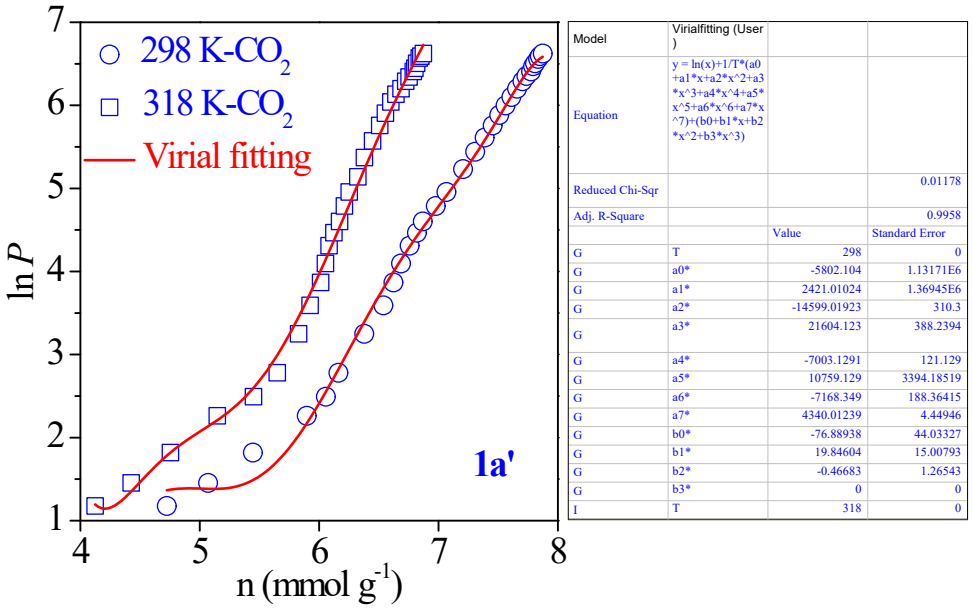

Model	Virialfitting (User)		
Equation	y = ln(x)+1/T*(a0+a1*x+a2*x^2+a3*x^3+a4*x^4+a5*x^5+a6*x^6+a7*x^7)+(b0+b1*x+b2*x^2+b3*x^3)		
Reduced Chi-Sqr			0.01178
Adj. R-Square			0.9958
		Value	Standard Error
G	T	298	0
G	a0*	-5802.104	1.13171E6
G	a1*	2421.01024	1.36945E6
G	a2*	-14599.01923	310.3
G	a3*	21604.123	388.2394
G	a4*	-7003.1291	121.129
G	a5*	10759.129	3394.18519
G	a6*	-7168.349	188.36415
G	a7*	4340.01239	4.44946
G	b0*	-76.88938	44.03327
G	b1*	19.84604	15.00793
G	b2*	-0.46683	1.26543
G	b3*	0	0
I	T	318	0

Figure S20. Virial fitting (lines) of the CO_2 adsorption isotherms over **1a'** measured at 298 and 318 K.

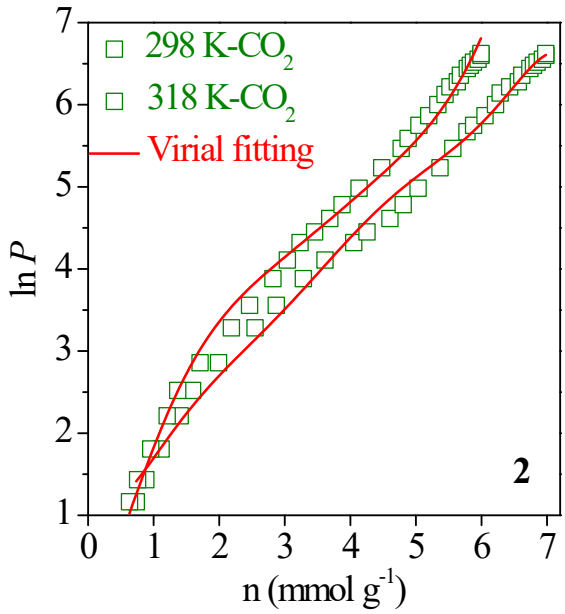

Model	Virialfitting (User)		
Equation	y = ln(x)+1/T*(a0+a1*x+a2*x^2+a3*x^3+a4*x^4+a5*x^5+a6*x^6+a7*x^7)+(b0+b1*x+b2*x^2+b3*x^3)		
Reduced Chi-Sqr			0.01688
Adj. R-Square			0.99402
		Value	Standard Error
G	T	298	0
G	a0*	-3422.01239	905.01035
G	a1*	674.1203	200.121
G	a2*	2270.10238	460.2304
G	a3*	-1413.01239	30.2123
G	a4*	6400.1239	39.23901
G	a5*	1576.123	45.29873
G	a6*	-888.123	4.12801
G	a7*	308.123	0.15309
G	b0*	-19.64907	2.41438
G	b1*	32.71485	1.60743
G	b2*	-10.33255	0.22528
G	b3*	1	0
I	T	318	0

Figure S21. Virial fitting (lines) of the CO_2 adsorption isotherms over **2** measured at 298 and 318 K.

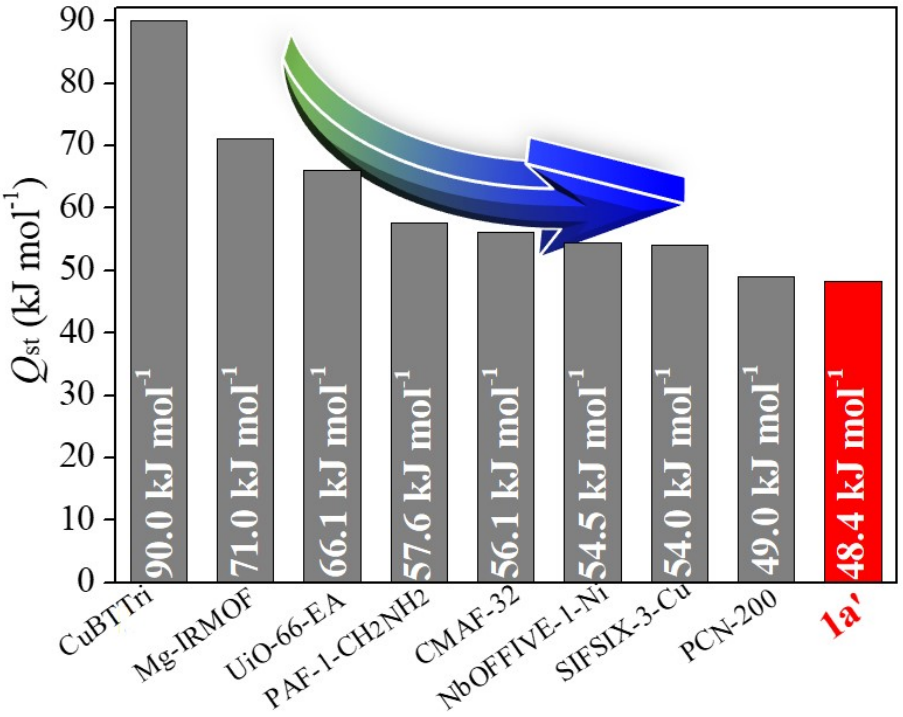

Figure S22. Comparison of Q_{st} over **1a'** and top-performing materials for CO_2 adsorption measured at similar conditions.

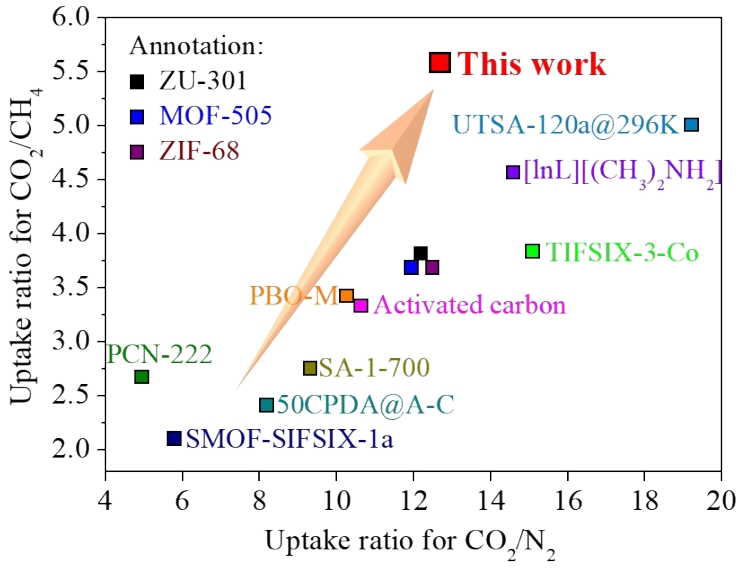

Figure S23. Comparison of uptake ratio CO_2/N_2 versus CO_2/CH_4 measured at 298 K and 1 bar. (The results were obtained from the single-gas adsorption isotherms).

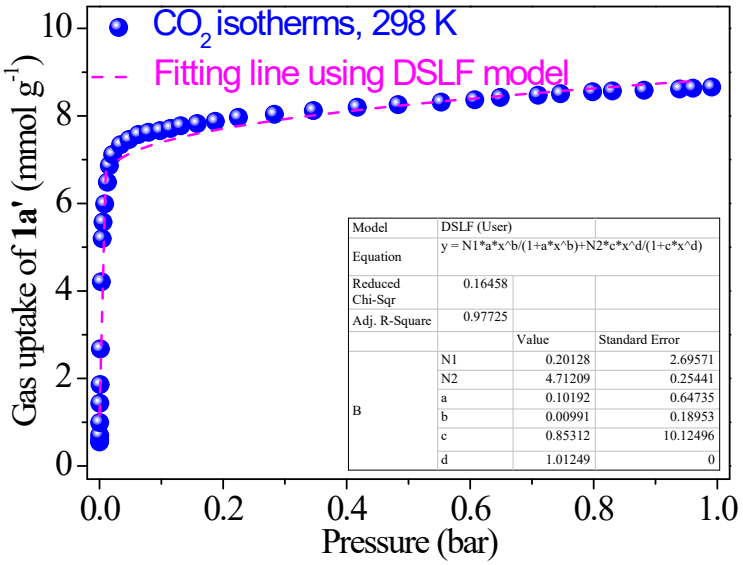

Figure S24. Isotherm fitting of CO_2 adsorption over **1a'** at 298 K and 1 bar.

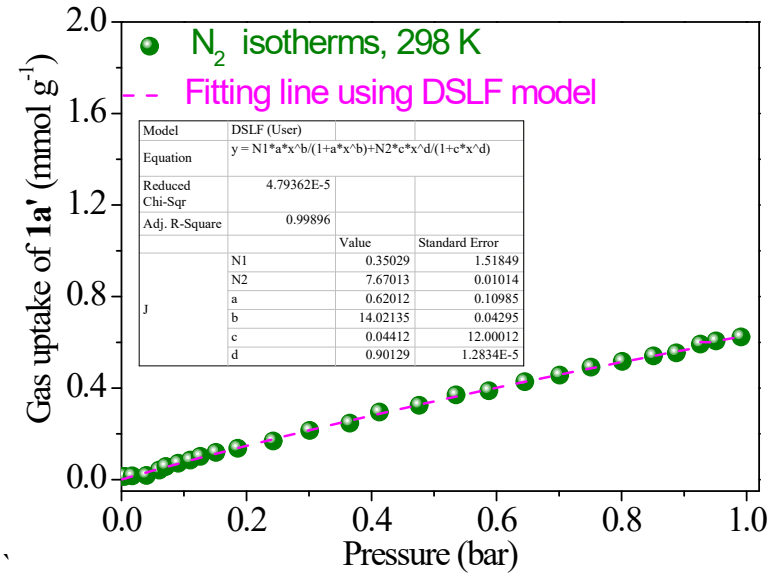

Figure S25. Isotherm fitting of N_2 adsorption over **1a'** at 298 K and 1 bar.

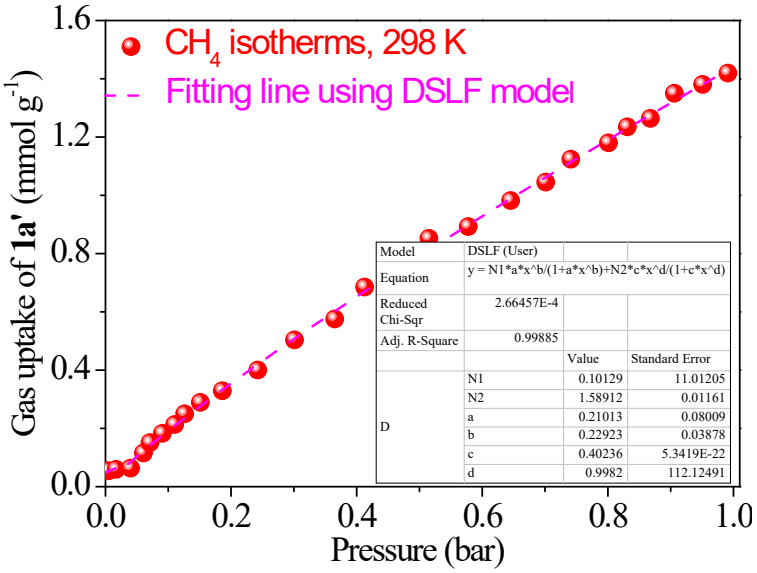

Figure S26. Isotherm fitting of CH_4 adsorption over **1a'** at 298 K and 1 bar.

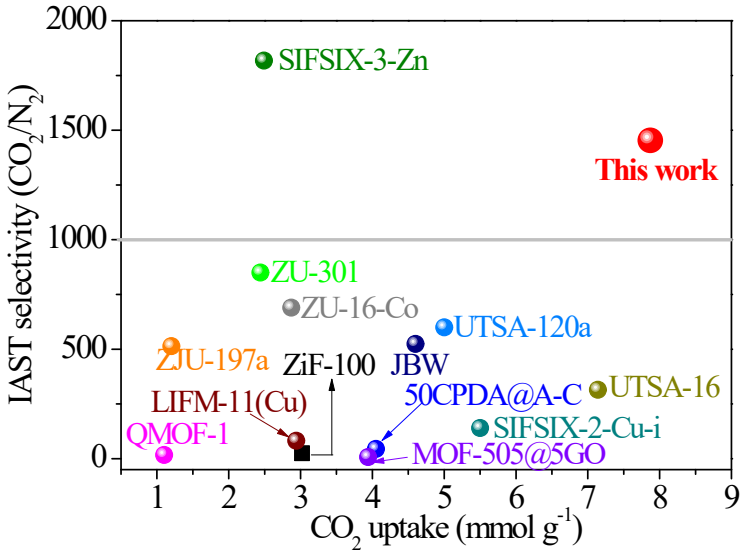

Figure S27. IAST selectivity of CO_2/N_2 (15/85, v/v) versus CO_2 uptake over selected **1a'** and the well-known MOF materials.

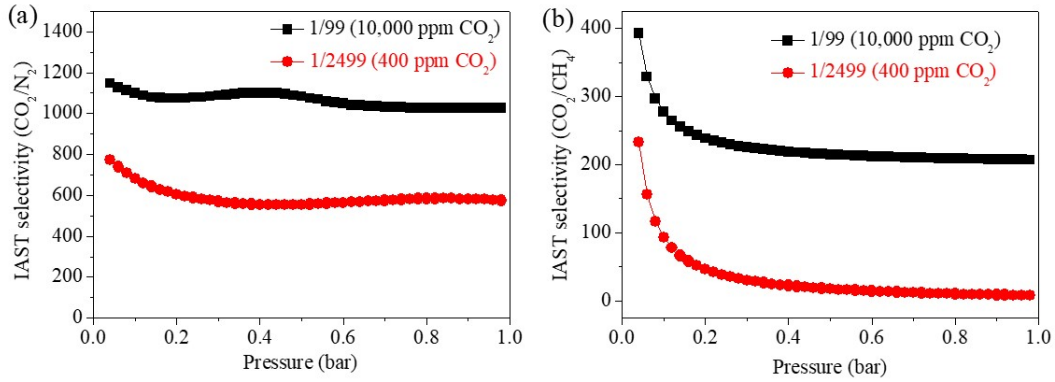

Figure S28. IAST calculations for 1/99 (containing 10, 000 ppm CO_2) and 1/2499 (containing 400 ppm CO_2) gas mixtures.

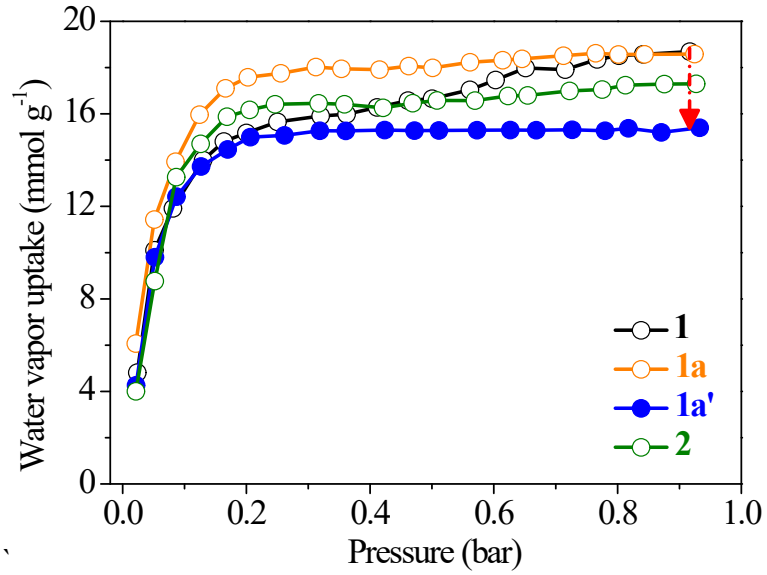

Figure S29. Adsorption isotherms of water vapor on the materials at 298 K and 1 bar.

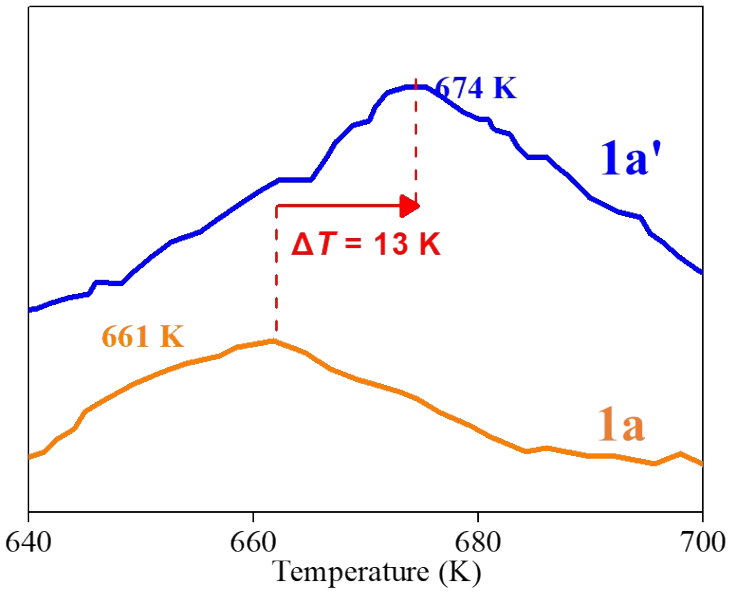

Figure S30. CO_2-TPD profiles over selected **1a** and **1a'**.

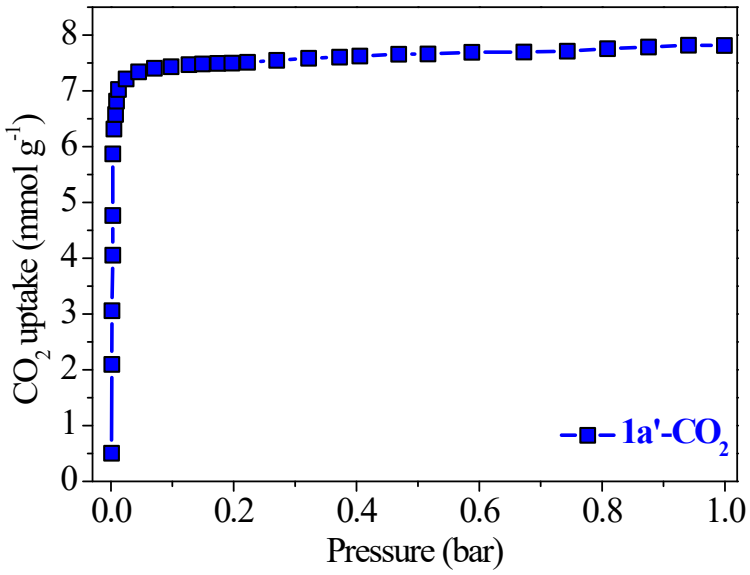

Figure S31. Simulated adsorption isotherms of CO_2 for **1a'** at 298 K and 1 bar.

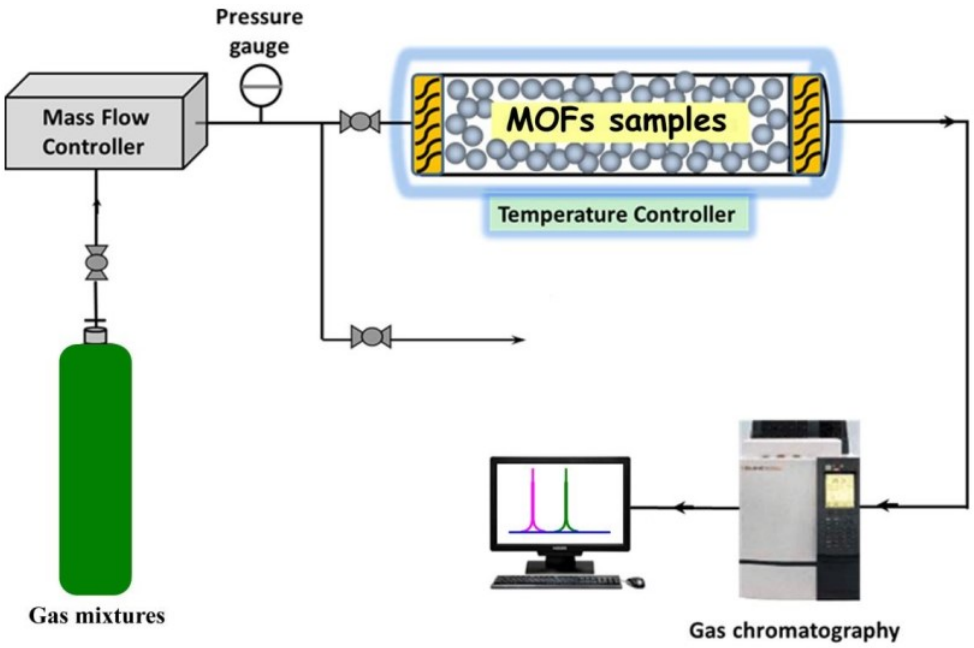

Figure S32. Schematic illustration of the apparatus for the breakthrough tests.

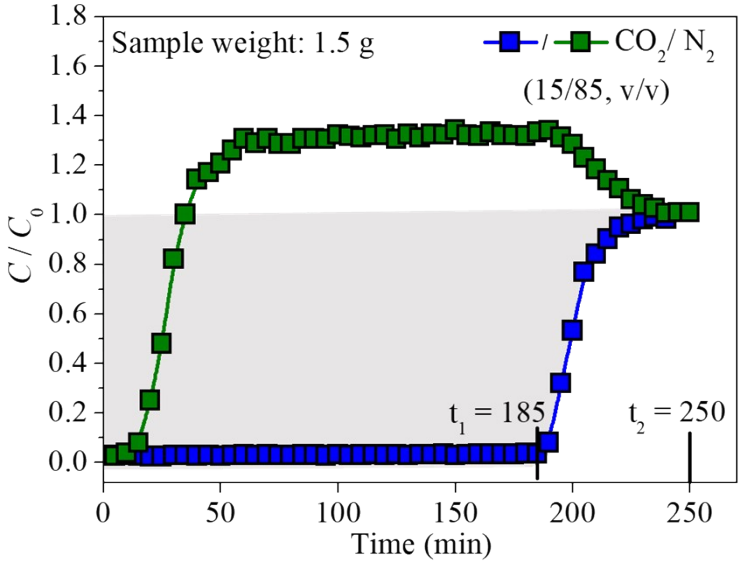

Figure S33. The calculation for captured amount of CO_2 during the breakthrough process of CO_2/N_2 (15/85, v/v) mixtures at 298 K.

(Conditions: total flow rate: 8 mL min^{-1}, temperature: 298 K, sample weight: 1.5 g)

Here, the flow rate of CO_2 (15%): q = 1.2 mL min^{-1} = 0.054 mmol min^{-1}. During the duration before breakthrough point (t_0~t_1), the captured amount of CO_2 in **1a'**, Q = qt = 0.054 mmol min^{-1} × 185 min = 9.99 mmol, corresponding to 6.66 mmol g^{-1}. Considering the continuous CO_2 adsorption during the mass transfer zone (t_1~t_2), the max amount of CO_2 during 0~250 min, $Q_{max} = q\int_0^{\infty}[C_i^0 - C_i(t)]dt$ = 10.85 mmol, corresponding to 162.0 L kg^{-1} (7.23 mmol g^{-1}), which is about 92% of its theoretical value under the same pressure (7.87 mmol g^{-1}).

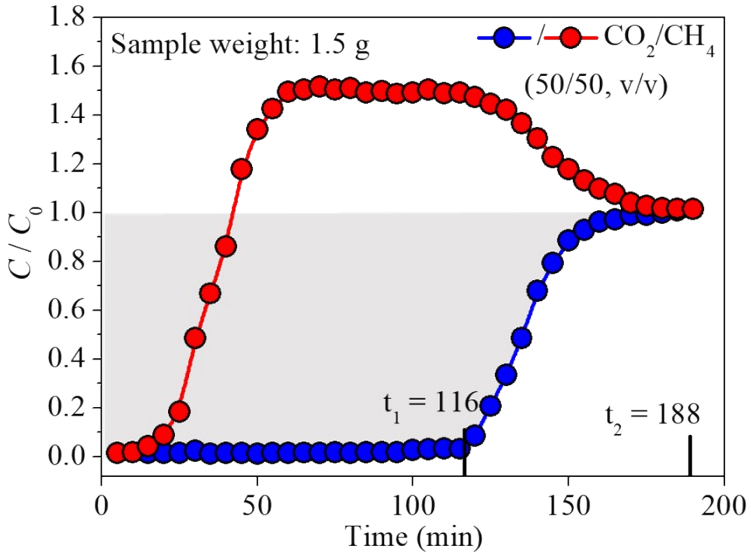

Figure S34. The calculation for captured amount of CO_2 during the breakthrough process of CO_2/CH_4 (50/50, v/v) mixtures at 298 K.

(Conditions: total flow rate: 4 mL min^{-1}, temperature: 298 K, sample weight: 1.5 g)

Here, the flow rate of CO_2 (50%): q = 2 mL min^{-1} = 0.089 mmol min^{-1}. During the duration before breakthrough point (t_0~t_1), the captured amount of CO_2 in **1a'**, Q = qt = 0.089 mmol min^{-1} × 116 min = 10.3 mmol, corresponding to 6.87 mmol g^{-1}. Considering the continuous CO_2 adsorption during the mass transfer zone (t_1~t_2), the max amount of CO_2 during 0~188 min, $Q_{max} = q\int_0^{\infty}[C_i^0 - C_i(t)]dt$ = 11.04 mmol, corresponding to 164.9 L kg^{-1} (7.36 mmol g^{-1}), which is about 94% of its theoretical value under the same pressure (7.87 mmol g^{-1}).

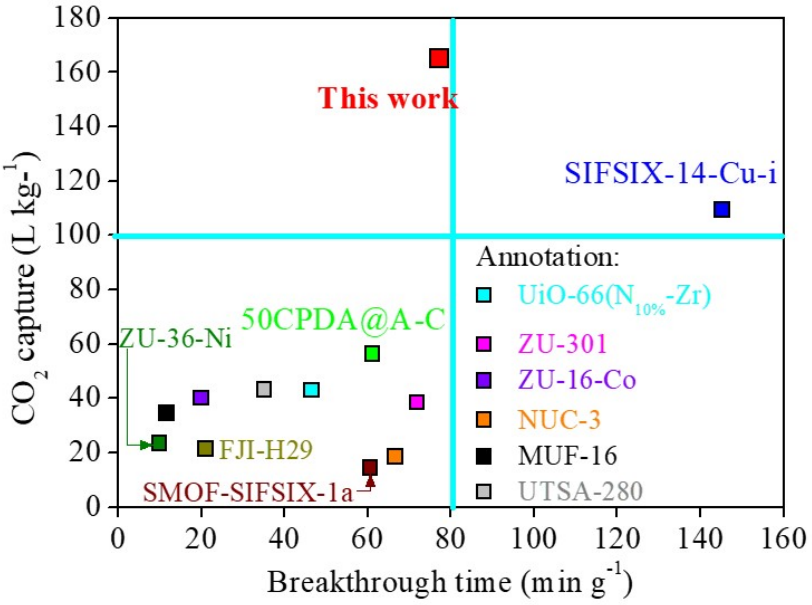

Figure S35. Comparison of CO_2 capture versus breakthrough time for CO_2/CH_4 breakthrough tests over **1a'** and well-known benchmark materials.

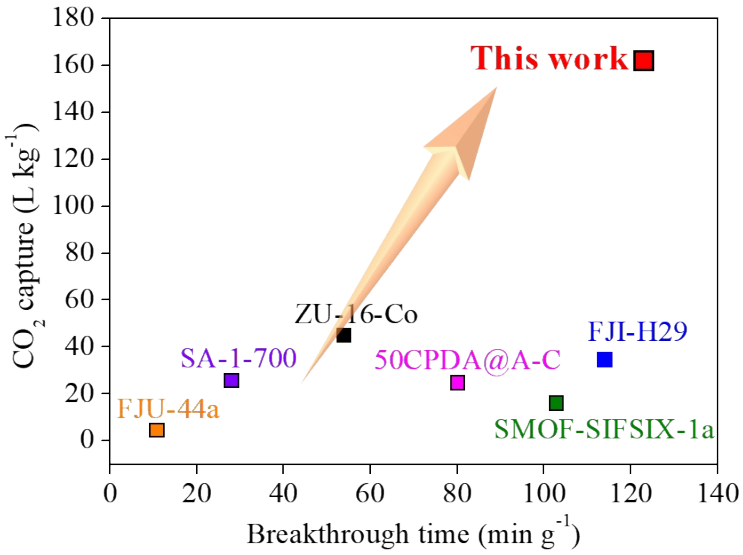

Figure S36. Comparison of CO_2 capture versus breakthrough time for CO_2/N_2 breakthrough tests over **1a'** and well-known adsorbents.

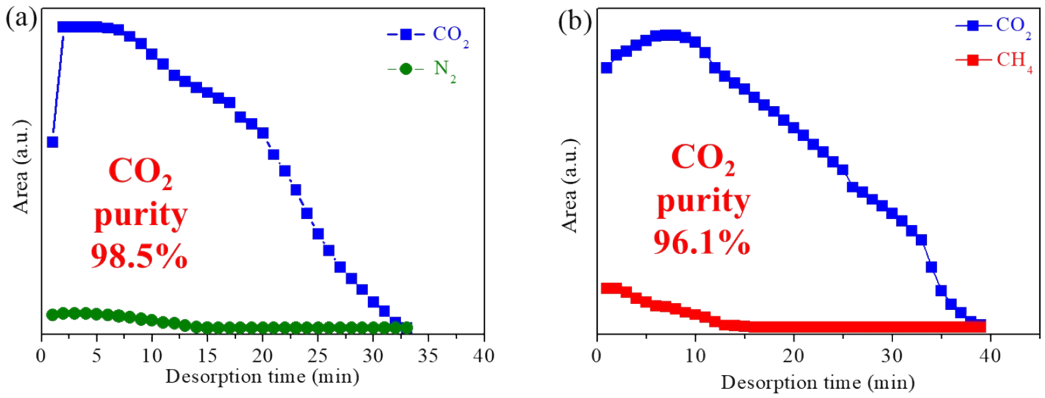

Figure S37. The CO_2 desorption curves of **1a'** for (a) CO_2/N_2 (18/85, v/v) and (b) CO_2/CH_4 (50/50, v/v) in breakthrough process.

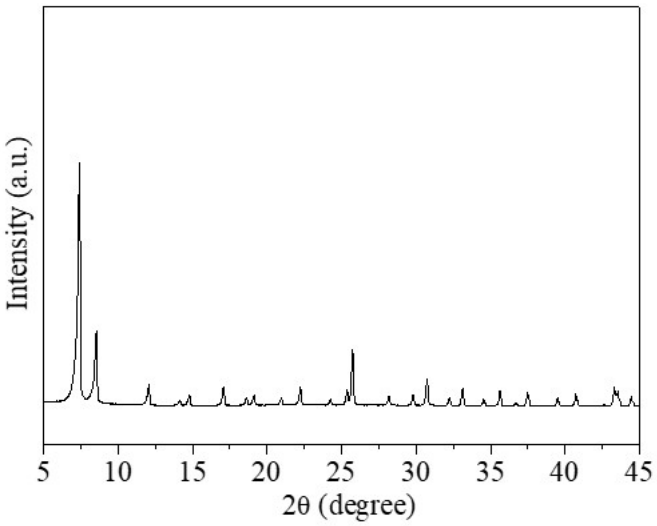

Figure S38. PXRD pattern of **1a'** after cycling tests.

4. Supporting Tables

Table S1. Physical properties of CO_2, N_2 and CH_4 used in this work.

Adsorbates	Kinetic diameter (Å)	Polarizability ($\times 10^{25}$ cm^3)	Dipole moment ($\times 10^{-10}$ nm)	Quadrupole moment ($\times 10^{-40}$ C·m^2)
CO_2	3.30	29.1	0	-13.4±0.4
N_2	3.64~3.8	17.4	0	-4.72±0.26
CH_4	3.76	25.9	0	0

Table S2. Crystallographic parameters and refinement details of selected materials.

Crystals	**1a**	**1a'@25 ℃**	**1a'@75 ℃**	**1a'@125 ℃**	**1a'@175 ℃**
Formula weight	2807.7	2807.3	2808.1	2807.6	2807.9
Crystal system	Trigonal	Trigonal	Trigonal	Trigonal	Trigonal
Space group	***R-3***	***R-3***	***R-3***	***R-3***	***R-3***
a (Å)	25.9088	25.9184	25.9063	25.9026	25.9061
c (Å)	6.8230	6.8242	6.8208	6.8303	6.8210
α (°)	90	90	90	90	90
β (°)	90	90	90	90	90
γ (°)	120	120	120	120	120
cell volume (Å^3)	4580.0	4584.2	4577.7	4582.8	4577.8
Calc. density (g cm^{-3})	1.168	1.174	1.172	1.169	1.172
R_P (%)	4.93	4.82	3.89	3.46	3.81
R_{WP} (%)	8.92	8.71	11.04	7.78	8.06

Table S3. Elemental analysis (EA) and ICP analysis of N and Co in yielding MOFs.

MOFs	Weight (G)	Yield (%)	Content (wt.%)		Amount of pyz[a]	Molar ratio of N/Co	
			N	Co	mmol	Experimental[b]	Theoretical[c]
1	0.7141	0.73	---	12.0	---	---	---
1a'	0.7514	0.71	2.50	10.8	0.67	0.9738	1

[a] represent the actual amount of pyz molecule in the yielding MOFs.

[b] represent the calculated molar ratio of N/Co in the MOFs through experimental method.

[c] represent the expected molar ratio of N/Co in the MOFs given that the unit formula in MOF was $[Co_2(dobdc)(pyz)]$.

Table S4. Structure data and pore parameters for these selected Co-MOF families. (Note: all the data were measured at 195 K and 1 bar, and CO_2 was used as the probe molecule)

Sample	S_{BET}[a] ($m^2\ g^{-1}$)	S_{micro}[b] ($m^2\ g^{-1}$)	S_{micro}/S_{bet} (%)
Simulated Co-MOF-74[e]	946	---	---
1	625	328	52.5
1a	825	581	70.4
1a'	1220	1087	89.1
2	786	509	64.8

[a] S_{BET} is the surface area of BET calculated from CO_2 isotherms at 195 K.

[b] S_{micro} is the surface area of microporous structure.

[c] V_t is the total volume.

[d] V_{micro} is microporous volume.

[e] the simulated data was calculated from the optimized cell model with CO_2 loading.

Table S5. Comparison of pore size information and CO_2 sorption results over comparable **1a'** and benchmark materials at 298 K and variable pressure.

Materials	Pore size Å	CO_2 uptake at different pressure (mmol g^{-1})			Ref.
		400 ppm (0.4 mbar)	10,000 ppm (10 mbar)	1 bar	
1	**7.0**	**0.12**	**0.91**	**7.28**	**This work**
1a	**7.3**	**0.64**	**3.42**	**6.83**	
1a'	**6.1**	**1.36**	**5.70**	**7.87**	
2	**7.8**	**0.19**	**1.28**	**6.98**	
Zu-16-Co	3.62	1.05	2.63	2.87	[2]
TIFSIX-3-Ni	3.40	0.67	1.75	2.32	
NbOFFIVE-1-Ni	3.21	1.30	1.71	2.20	[3]
SIFSIX-2-Cu-i	4.90	0.068	0.19	4.71	[4]
SIFSIX-14-Cu-i	3.60	N.G.[a]	1.72	4.70	[5]
dptz-$CuTiF_6$	4.5 ~ 6.0	N.R.[b]	2.10	4.51	[6]
SIFSIX-3-Cu	3.52	1.24	2.34	2.50	[7]
SIFSIX-18-Ni-β	N.R.[b]	0.4[c]	2.2	2.5	[8]
SIFSIX-3-Ni	N.R.[b]	N.R.[b]	N.R.[b]	2.5	[9]

[a] N.G. represent the value was negligible.

[b] N.R. represent the value was not reported.

Table S6. Summary of the adsorption capacity and uptake ratio for CO_2, N_2 and CH_4 in various CO_2-based sorbents at 298 K and 1 bar, respectively.

Adsorbents	Adsorption capacity at 1 bar (mmol g^{-1})			Uptake ratio at 1 bar		**Ref.**
	CO_2	N_2	CH_4	CO_2/N_2	CO_2/CH_4	
1a'	7.87	0.62	1.41	12.69	5.58	**This work**
ZU-301	2.44	0.20	0.64	12.20	3.81	[10]
TIFSIX-3-Co	2.87	0.19	0.75	15.10	3.83	[11]
MOF-505	2.87	0.24	0.78	11.96	3.68	[12]
UTSA-120a	5.0[a]	0.26[b]	1.0[b]	19.23	5.00	[13]
Activated carbon	2.13	0.20	0.64	10.65	3.33	[14]
PBO-M	2.67	0.26	0.78	10.27	3.42	[15]
SA-1-700	4.20	0.45	1.53	9.33	2.75	[16]
SMOF-SIFSIX-1a	1.51	0.26	0.72	5.80	2.10	[17]
ZIF-68	2.50	0.20	0.68	12.50	3.68	[18]
$[InL][(CH_3)_2NH_2]$	1.46	0.10	0.32	14.60	4.56	[19]
PCN-222	13.9	2.80	5.20	4.96	2.67	[20]
50CPDA@A-C	4.10	0.50	1.70	8.20	2.41	[21]

[a] referred to the value obtained from the single-gas isotherm at 296 K and 1 bar.

Table S7. Dual-site Langmuir -Freundlich parameters fits for CO_2, N_2 and CH_4 of **1a'**.

		Site A			**Site B**		
		N_1	a	b	N_2	c	d
		mol kg^{-1}	Pa^{-vA}	dimensionless	mol kg^{-1}	Pa^{-vA}	dimensionless
1a'	CO_2	0.2013	0.1019	0.0099	4.712	0.8531	1.013
	N_2	0.3503	0.6201	14.02	7.670	0.04412	0.9013
	CH_4	0.1013	0.2101	0.2292	1.589	0.4024	0.9982

Table S8. Summary of the CO_2 adsorption, selectivities for CO_2/CH_4 (50/50, v/v) and CO_2/N_2 (15/85, v/v) in various porous materials.

Adsorbents	Conditions		CO_2 uptakes[a] (mmol g^{-1})	IAST selectivity		Ref.
	T (K)	P (bar)		CO_2/CH_4 (50/50, v/v)	CO_2/N_2 (15/85, v/v)	
1a'	**298**	**1**	**7.87**	**494**	**1454**	**This work**
UTSA-120a	296	1	5.0	100	600	[13]
ZU-301	298	1	2.44	111	850	[10]
50CPDA@A-C	298	1	4.05	7.6	45.0	[21]
ZJU-197a	298	1	1.2	53	514.1	[22]
QMOF-1	298	1	1.1	6.4	17.2	[23]
MOF-505@5GO	298	1	3.94	27.8	7.6	[12]
UTSA-16	298	1	7.14	29.8	314.7	[24]
ZU-16-Co	298	1	2.87	120	690	[25]
NKU-521	298	1	3.7	N.R.[b]	40	[26]
ZIF-100	273	1	3.02	5.9	25	[27]
LIFM-11(Cu)	298	1	2.94	17.2	81.9	[28]
SIFSIX-3-Zn	298	1	2.49	231	1818	[29]
SIFSIX-2-Cu-i	298	1	5.50	33	140	[29]
JBW	296	1	4.60	685.5	524.4	[30]

[a] referred to the value obtained from the single-gas isotherm.

[b] N.R. referred to the values were not reported.

Table S9. Comparison of determined CO_2 and H_2O diffusion parameters for diffusivity at 298 K and 0.1 bar.

Adsorbates	Adsorbents	D_M/r_c^2 ($\times 10^{-3}$ s^{-1})	D_M ($\times 10^{-15}$ m^2 s^{-1})
CO_2	**1a**	8.71	**3.68**
	1a'	45.2	**19.1**
H_2O	**1a**	4.95	**2.09**
	1a'	2.55	**1.08**

Table S10. Comparison of simulated CO_2 and H_2O diffusion parameters for diffusivity.

Adsorbates	Adsorbents	Fitting *K* value ($\times 10^{-7}$)	D_S ($\times 10^{-15}$ m^2 s^{-1})
CO_2	**1a**	24.5	4.08
	1a'	147	24.5
H_2O	**1a**	14.2	2.37
	1a'	7.35	1.23

Table S11. List of atomic positions for CO_2-loaded **1a'** obtained from DFT calculations.

Atom	x/a	y/b	z/c	Atom	x/a	y/b	z/c
C1	0.45655	0.3263	0.1351	O28	0.34438	0.37387	0.05734
C2	0.4368	0.3303	0.1821	Co29	0.35758	0.34772	0.10292
O3	0.4479	0.31735	0.0778	C30	0.3263	0.36975	0.19823
O4	0.48895	0.2928	0.05377	C31	0.3303	0.3935	0.15123
Co5	0.47575	0.31895	0.00819	O32	0.31735	0.36945	0.25553
C6	0.28988	0.49297	0.24621	O33	0.31705	0.31495	0.06637
C7	0.32778	0.43902	0.13654	O34	0.2928	0.30385	0.27957
C8	0.32488	0.41577	0.17504	Co35	0.31895	0.3432	0.32514
O9	0.28123	0.48402	0.18891	C36	0.29692	0.28988	0.08712
O10	0.33543	0.48372	0.04474	C37	0.38877	0.32778	0.19679
O11	0.32228	0.45947	0.16488	C38	0.40912	0.32488	0.15829
Co12	0.30908	0.48561	0.1193	O39	0.29722	0.28123	0.14442
C13	0.34037	0.46358	0.02399	O40	0.35172	0.33543	0.28859
C14	0.33637	0.43983	0.07099	O41	0.36282	0.32228	0.16846
O15	0.34932	0.46388	0.30002	Co42	0.32347	0.30908	0.21403
Co16	0.34772	0.49014	0.23042	O43	0.5021	0.31705	0.26697
O17	0.31495	0.4979	0.26697	C44	0.50703	0.29692	0.24621
C18	0.44457	0.33888	0.24766	C45	0.56098	0.38877	0.13654
C19	0.42422	0.34178	0.28616	C46	0.58423	0.40912	0.17504
O20	0.48162	0.33123	0.15586	O47	0.51598	0.29722	0.18891
O21	0.47052	0.34438	0.27599	O48	0.51628	0.35172	0.04474
C22	0.37678	0.34037	0.30934	O49	0.54053	0.36282	0.16488
C23	0.39653	0.33637	0.26234	Co50	0.51439	0.32347	0.1193
C24	0.33888	0.39432	0.08568	C51	0.53642	0.37678	0.02399
C25	0.34178	0.41757	0.04718	C52	0.56017	0.39653	0.07099
O26	0.38543	0.34932	0.03331	O53	0.53612	0.38543	0.30002

O27	0.33123	0.34962	0.17748	Co54	0.50986	0.35758	0.23042
Atom	x/a	y/b	z/c	Atom	x/a	y/b	z/c
C55	0.60568	0.44457	0.08568	C82	0.43983	0.60347	0.26234
C56	0.58243	0.42422	0.04718	O83	0.46388	0.61457	0.03331
O57	0.65038	0.48162	0.17748	Co84	0.49014	0.64242	0.10292
O58	0.62613	0.47052	0.05734	C85	0.62322	0.65963	0.02399
C59	0.63025	0.45655	0.19823	C86	0.60347	0.66363	0.07099
C60	0.6065	0.4368	0.15123	C87	0.66112	0.60568	0.24766
O61	0.63055	0.4479	0.25553	C88	0.65822	0.58243	0.28616
O62	0.69615	0.48895	0.27957	O89	0.61457	0.65068	0.30002
Co63	0.65681	0.47575	0.32514	O90	0.66877	0.65038	0.15586
C64	0.39432	0.55543	0.24766	O91	0.65562	0.62613	0.27599
C65	0.41757	0.57578	0.28616	Co92	0.64242	0.65228	0.23042
O66	0.34962	0.51838	0.15586	C93	0.6737	0.63025	0.1351
O67	0.37387	0.52948	0.27599	C94	0.6697	0.6065	0.1821
C68	0.36975	0.54345	0.1351	O95	0.68265	0.63055	0.0778
C69	0.3935	0.5632	0.1821	O96	0.68295	0.68505	0.26697
O70	0.36945	0.5521	0.0778	O97	0.7072	0.69615	0.05377
O71	0.30385	0.51105	0.05377	Co98	0.68105	0.65681	0.00819
Co72	0.3432	0.52425	0.00819	C99	0.70308	0.71012	0.24621
O73	0.4979	0.68295	0.06637	C100	0.61123	0.67222	0.13654
C74	0.49297	0.70308	0.08712	C101	0.59088	0.67512	0.17504
C75	0.43902	0.61123	0.19679	O102	0.70278	0.71877	0.18891
C76	0.41577	0.59088	0.15829	O103	0.64828	0.66457	0.04474
O77	0.48402	0.70278	0.14442	O104	0.63718	0.67772	0.16488
O78	0.48372	0.64828	0.28859	Co105	0.67653	0.69092	0.1193
O79	0.45947	0.63718	0.16846	C106	0.54345	0.6737	0.19823
Co80	0.48561	0.67653	0.21403	C107	0.5632	0.6697	0.15123
C81	0.46358	0.62322	0.30934	O108	0.5521	0.68265	0.25553

Atom	x/a	y/b	z/c	Atom	x/a	y/b	z/c
O109	0.51105	0.7072	0.27957	O137	0.32228	0.45947	0.49821
Co110	0.52425	0.68106	0.32514	Co138	0.30908	0.48561	0.45264
C111	0.71012	0.50703	0.08712	C139	0.34037	0.46358	0.35732
C112	0.67222	0.56098	0.19679	C140	0.33637	0.43983	0.40432
C113	0.67512	0.58423	0.15829	O141	0.34932	0.46388	0.63336
O114	0.71877	0.51598	0.14442	Co142	0.34772	0.49014	0.56375
O115	0.66457	0.51628	0.28859	O143	0.31495	0.4979	0.6003
O116	0.67772	0.54053	0.16846	C144	0.44457	0.33888	0.58099
Co117	0.69092	0.51439	0.21403	C145	0.42422	0.34178	0.61949
C118	0.65963	0.53642	0.30934	O146	0.48162	0.33123	0.48919
C119	0.66363	0.56017	0.26234	O147	0.47052	0.34438	0.60932
O120	0.65068	0.53612	0.03331	C148	0.37678	0.34037	0.64268
Co121	0.65228	0.50986	0.10292	C149	0.39653	0.33637	0.59568
O122	0.68505	0.5021	0.06637	C150	0.33888	0.39432	0.41901
C123	0.55543	0.66112	0.08568	C151	0.34178	0.41757	0.38051
C124	0.57578	0.65822	0.04718	O152	0.38543	0.34932	0.36664
O125	0.51838	0.66877	0.17748	O153	0.33123	0.34962	0.51081
O126	0.52948	0.65562	0.05734	O154	0.34438	0.37387	0.39068
C127	0.45655	0.3263	0.46843	Co155	0.35758	0.34772	0.43625
C128	0.4368	0.3303	0.51543	C156	0.3263	0.36975	0.53157
O129	0.4479	0.31735	0.41113	C157	0.3303	0.3935	0.48457
O130	0.48895	0.2928	0.3871	O158	0.31735	0.36945	0.58887
Co131	0.47575	0.31895	0.34153	O159	0.31705	0.31495	0.3997
C132	0.28988	0.49297	0.57954	O160	0.2928	0.30385	0.6129
C133	0.32778	0.43902	0.46988	Co161	0.31895	0.3432	0.65847
C134	0.32488	0.41577	0.50838	C162	0.29692	0.28988	0.42046
O135	0.28123	0.48402	0.52224	C163	0.38877	0.32778	0.53012

O136	0.33543	0.48372	0.37808	C164	0.40912	0.32488	0.49162
Atom	x/a	y/b	z/c	Atom	x/a	y/b	z/c
O165	0.29722	0.28123	0.47776	O193	0.37387	0.52948	0.60932
O166	0.35172	0.33543	0.62192	C194	0.36975	0.54345	0.46843
O167	0.36282	0.32228	0.50179	C195	0.3935	0.5632	0.51543
Co168	0.32347	0.30908	0.54736	O196	0.36945	0.5521	0.41113
O169	0.5021	0.31705	0.6003	O197	0.30385	0.51105	0.3871
C170	0.50703	0.29692	0.57954	Co198	0.3432	0.52425	0.34153
C171	0.56098	0.38877	0.46988	O199	0.4979	0.68295	0.3997
C172	0.58423	0.40912	0.50838	C200	0.49297	0.70308	0.42046
O173	0.51598	0.29722	0.52224	C201	0.43902	0.61123	0.53012
O174	0.51628	0.35172	0.37808	C202	0.41577	0.59088	0.49162
O175	0.54053	0.36282	0.49821	O203	0.48402	0.70278	0.47776
Co176	0.51439	0.32347	0.45264	O204	0.48372	0.64828	0.62192
C177	0.53642	0.37678	0.35732	O205	0.45947	0.63718	0.50179
C178	0.56017	0.39653	0.40432	Co206	0.48561	0.67653	0.54736
O179	0.53612	0.38543	0.63336	C207	0.46358	0.62322	0.64268
Co180	0.50986	0.35758	0.56375	C208	0.43983	0.60347	0.59568
C181	0.60568	0.44457	0.41901	O209	0.46388	0.61457	0.36664
C182	0.58243	0.42422	0.38051	Co210	0.49014	0.64242	0.43625
O183	0.65038	0.48162	0.51081	C211	0.62322	0.65963	0.35732
O184	0.62613	0.47052	0.39068	C212	0.60347	0.66363	0.40432
C185	0.63025	0.45655	0.53157	C213	0.66112	0.60568	0.58099
C186	0.6065	0.4368	0.48457	C214	0.65822	0.58243	0.61949
O187	0.63055	0.4479	0.58887	O215	0.61457	0.65068	0.63336
O188	0.69615	0.48895	0.6129	O216	0.66877	0.65038	0.48919
Co189	0.65681	0.47575	0.65847	O217	0.65562	0.62613	0.60932
C190	0.39432	0.55543	0.58099	Co218	0.64242	0.65228	0.56375
C191	0.41757	0.57578	0.61949	C219	0.6737	0.63025	0.46843

O192	0.34962	0.51838	0.48919	C220	0.6697	0.6065	0.51543
Atom	x/a	y/b	z/c	Atom	x/a	y/b	z/c
O221	0.68265	0.63055	0.41113	C249	0.57578	0.65822	0.38051
O222	0.68295	0.68505	0.6003	O250	0.51838	0.66877	0.51081
O223	0.7072	0.69615	0.3871	O251	0.52948	0.65562	0.39068
Co224	0.68105	0.65681	0.34153	N252	0.39077	0.49921	0.21354
C225	0.70308	0.71012	0.57954	C253	0.39484	0.47529	0.20873
C226	0.61123	0.67222	0.46988	C254	0.4237	0.4799	0.20252
C227	0.59088	0.67512	0.50838	N255	0.44723	0.50821	0.2014
O228	0.70278	0.71877	0.52224	C256	0.44317	0.53213	0.20622
O229	0.64828	0.66457	0.37808	C257	0.41431	0.52753	0.21243
O230	0.63718	0.67772	0.49821	N258	0.38993	0.50396	0.54631
Co231	0.67653	0.69092	0.45264	C259	0.394	0.48004	0.5415
C232	0.54345	0.6737	0.53157	C260	0.42286	0.48465	0.53529
C233	0.5632	0.6697	0.48457	N261	0.4464	0.51296	0.53418
O234	0.5521	0.68265	0.58887	C262	0.44233	0.53688	0.53899
O235	0.51105	0.7072	0.6129	C263	0.41347	0.53228	0.5452
C236	0.71012	0.50703	0.42046	N264	0.55758	0.55888	0.58986
C237	0.67222	0.56098	0.53012	C265	0.58546	0.56265	0.58523
C238	0.67512	0.58423	0.49162	C266	0.61016	0.59138	0.58835
O239	0.71877	0.51598	0.47776	N267	0.60591	0.61508	0.59599
O240	0.66457	0.51628	0.62192	C268	0.57804	0.61131	0.60062
O241	0.67772	0.54053	0.50179	C269	0.55333	0.58259	0.5975
Co242	0.69092	0.51439	0.54736	N270	0.56135	0.5577	0.21113
C243	0.65963	0.53642	0.64268	C271	0.58923	0.56147	0.2065
C244	0.66363	0.56017	0.59568	C272	0.61393	0.5902	0.20963
O245	0.65068	0.53612	0.36664	N273	0.60968	0.6139	0.21726
Co246	0.65228	0.50986	0.43625	C274	0.58181	0.61013	0.2219
O247	0.68505	0.5021	0.3997	C275	0.5571	0.5814	0.21877

C248	0.55543	0.66112	0.41901	N276	0.50736	0.38463	0.57564

Atom	x/a	y/b	z/c	Atom	x/a	y/b	z/c
C277	0.53256	0.4114	0.58459	O288	0.52531	0.45423	0.42734
C278	0.53045	0.43718	0.58998	C289	0.50066	0.48623	0.43458
N279	0.50324	0.43505	0.5862	O290	0.47602	0.51823	0.44184
C280	0.47804	0.40829	0.57726	O291	0.46696	0.45997	0.22233
C281	0.48014	0.38251	0.57187	C292	0.44168	0.44567	0.17366
N282	0.51042	0.38583	0.22175	O293	0.41639	0.43137	0.125
C283	0.53545	0.41315	0.22337				
C284	0.53298	0.43865	0.21603				
N285	0.50559	0.43571	0.20742				
C286	0.48057	0.40838	0.20581				
C287	0.48303	0.38289	0.21314				
O288	0.52531	0.45423	0.42734				
C289	0.50066	0.48623	0.43458				
O290	0.47602	0.51823	0.44184				
O291	0.46696	0.45997	0.22233				
C292	0.44168	0.44567	0.17366				
O293	0.41639	0.43137	0.125				
C277	0.53256	0.4114	0.58459				
C278	0.53045	0.43718	0.58998				
N279	0.50324	0.43505	0.5862				
C280	0.47804	0.40829	0.57726				
C281	0.48014	0.38251	0.57187				
N282	0.51042	0.38583	0.22175				
C283	0.53545	0.41315	0.22337				
C284	0.53298	0.43865	0.21603				
N285	0.50559	0.43571	0.20742				
C286	0.48057	0.40838	0.20581				

C287	0.48303	0.38289	0.21314

Table S12. Calculated adsorption energies (in kJ mol^{-1}) for CO_2 molecule at two sites in **1a'** as determined from periodic DFT calculations. (**Site I** and **Site II** correspond to the two geometrical adsorption sites in the channel of **1a'**)

Adsorbents	Adsorbates	Sites	ΔE_B (kJ mol^{-1})	Total ΔE_B (kJ mol^{-1})	Experimental Q_{st} (kJ mol^{-1})
1a'	CO_2	I	**19.6**	**47.7**	47.0
		II	**28.1**		

Table S13. Breakthrough tests of CO_2/CH_4 for **1a'** and well-known benchmark materials.

Adsorbents	Sample weight (g)	Flow rate (mL min^{-1})	T [a] (K)	Feed ratio (v/v)	BT [b] (min g^{-1})	CO_2 captured [c]		Ref.[d]
						(mmol g^{-1})	(L kg^{-1})	
1a'	1.5	4	298	50/50	77.3	7.36	164.9	**This work**
ZU-36-Ni	0.63	4	298	50/50	10	1.04	23.3	31
ZU-301	1.092	1	313	50/50	72	1.71	38.3	10
ZU-16-Co	0.7	4	298	50/50	20	1.78	39.9	2
NUC-3	0.48	2	298	50/50	66.7	0.82	18.4	32
SMOF-SIFSIX-1a	0.9717	0.32	298	50/50	60.7	0.64	14.3	33
FJI-H29	0.5232	2	293	40/60	21.2	0.94	21.1	34
MUF-16	0.9	6	298	50/50	11.8	1.53	34.3	35
SIFSIX-14-Cu-i	0.238	1.5	298	50/50	145.4	4.87	109.1	36
50CPDA@A-C	0.212	2	298	50/50	61.3[d]	2.51	56.2	37
SA-1-700	0.8	2	298	40/60	15.1	N.R.[e]	N.C.[f]	38
MIP-202	1.2	1	298	50/50	2.0[e]	N.R.[e]	N.C.[f]	39
UTSA-120a	0.582	2	298	50/50	36	N.R.[e]	N.C.[f]	40
ZU-66	0.43	1.94	298	50/50	65.1	N.R.[e]	N.C.[f]	41
PBO-M	0.3	5	273	50/50	40[d]	N.R.[e]	N.C.[f]	42
Cu-1	0.744	2	298	50/50	52.4	N.R.[e]	N.C.[f]	43

[a] represent the temperature (T, K) in the operating breakthrough process.

[b] represent breakthrough time (BT, min g^{-1}).

[c] represent CO_2 capture (mmol g^{-1}) calculated from the breakthrough curve.

[d] Estimated value based on the tested breakthrough curve.

[e] represent not reported.

[f] represent not calculated.

Table S14. Breakthrough tests of CO_2/N_2 for **1a'** and well-known benchmark materials.

Adsorbents	Sample weight (g)	Flow rate (mL min^{-1})	T[a] (K)	Feed ratio (v/v)	BT[b] (min g^{-1})	CO_2 captured [c] (mmol g^{-1})	CO_2 captured [c] (L kg^{-1})	Ref.[d]
1a'	1.5	8	298	15/85	123	7.23	162	**This work**
ZU-16-Co	0.7	5	298	15/85	54.0	1.99	44.6	31
SMOF-SIFSIX-1a	0.9717	0.7	298	15/85	103	0.70	15.7	17
FJI-H29	0.5232	2	293	15/85	114.2	1.53	34.3	32
FJU-44a	0.5	2	296	15/85	11	0.183	4.10	44
50CPDA@A-C	0.212	2	298	15/85	80.2[d]	1.09	24.4	37
SA-1-700	0.8	2	298	15/85	28.1	1.14	25.5	16
SC-6	0.6	1	298	30/70	46.7	N.R.[e]	N.C.[f]	45
ZU-36-Ni	0.63	4	298	15/85	27[d]	N.R.[e]	N.C.[f]	31
ZU-301	1.092	1	313	15/85	165	N.R.[e]	N.C.[f]	10
MIP-202	1.2	1	298	15/85	2.7[d]	N.R.[e]	N.C.[f]	46
UTSA-120a	0.582	2	298	15/85	84	N.R.[e]	N.C.[f]	40
ZU-66	0.43	2.05	298	15/85	65[d]	N.R.[e]	N.C.[f]	41
SIFSIX-14-Cu-i	0.238	1.0	273	15/85	84[d]	N.R.[e]	N.C.[f]	36
PBO-M	0.3	5	273	15/85	50[d]	N.R.[e]	N.C.[f]	47
Cu-1	0.744	2	298	10/90	44.3	N.R.[e]	N.C.[f]	43

[a] represent the temperature (T, K) in the operating breakthrough process.

[b] represent breakthrough time (BT, min g^{-1}).

[c] represent CO_2 capture (mmol g^{-1}) calculated from the breakthrough curve.

[d] Estimated value based on the tested breakthrough curve.

[e] represent not reported.

[f] represent not calculated.

References

1 L. Li, H. Wen, C. He, R. Lin, R. Krishna, H. Wu, W. Zhou, J. Li, B. Li and B. Chen, *Angew. Chem. Int. Edit.*, 2018, **57**, 15183-15188.

2 Z. Zhang, Q. Ding, J. Cui, X. Cui and H. Xing, *SCIENCE CHINA-MATERIALS*, 2021, **64**, 691-697.

3 P.M. Bhatt, Y. Belmabkhout, A. Cadiau, K. Adil, O. Shekhah, A. Shkurenko, L.J. Barbour and M. Eddaoudi, *J. Am. Chem. Soc.*, 2016, **138**, 9301-9307.

4 P. Nugent, Y. Belmabkhout, S.D. Burd, A.J. Cairns, R. Luebke, K. Forrest, T. Pham, S. Ma, B. Space, L. Wojtas, M. Eddaoudi and M.J. Zaworotko, *Nature*, 2013, **495**, 80-84.

5 M. Jiang, B. Li, X. Cui, Q. Yang, Z. Bao, Y. Yang, H. Wu, W. Zhou, B. Chen and H. Xing, *ACS Appl. Mater. Inter.*, 2018, **10**, 16628-16635.

6 W. Liang, P.M. Bhatt, A. Shkurenko, K. Adil, G. Mouchaham, H. Aggarwal, A. Mallick, A. Jamal, Y. Belmabkhout and M. Eddaoudi, *CHEM*, 2019, **5**, 950-963.

7 O. Shekhah, Y. Belmabkhout, Z. Chen, V. Guillerm, A. Cairns, K. Adil and M. Eddaoudi, *Nat. Commun.*, 2014, **5**.

8 S. Mukherjee, N. Sikdar, D. O'Nolan, D.M. Franz, V. Gascon, A. Kumar, N. Kumar, H.S. Scott, D.G. Madden, P.E. Kruger, B. Space and M.J. Zaworotko, *SCIENCE ADVANCES*, 2019, **5**.

9 D.G. Madden, A.B. Albadarin, D. O'Nolan, P. Cronin, J.J. Perry, S. Solomon, T. Curtin, M. Khraisheh, M.J. Zaworotko and G.M. Walker, *ACS Appl. Mater. Inter.*, 2020, **12**, 33759-33764.

10 C. Yu, Q. Ding, J. Hu, Q. Wang, X. Cui and H. Xing, *Chem. Eng. J.*, 2021, **405**.

11 Z. Zhang, Q. Ding, J. Cui, X. Cui and H. Xing, *SCIENCE CHINA-MATERIALS*, 2021, **64**, 691-697.

12 Y. Chen, D. Lv, J. Wu, J. Xiao, H. Xi, Q. Xia and Z. Li, *Chem. Eng. J.*, 2017, **308**, 1065-1072.

13 H. Wen, C. Liao, L. Li, A. Alsalme, Z. Alothman, R. Krishna, H. Wu, W. Zhou, J. Hu and B. Chen, *J. Mater. Chem. A*, 2019, **7**, 3128-3134.

14 J. Park, N.F. Attia, M. Jung, M.E. Lee, K. Lee, J. Chung and H. Oh, *Energy*, 2018, **158**, 9-16.

15 B. Zhang, J. Yan and Z. Wang, *J. Phys. Chem. C*, 2018, **122**, 12831-12838.

16 F. Yang, J. Wang, L. Liu, P. Zhang, W. Yu, Q. Deng, Z. Zeng and S. Deng, *ACS Sustain. Chem. Eng.*, 2018, **6**, 15550-15559.

17 J. Dai, D. Xie, Y. Liu, Z. Zhang, Y. Yang, Q. Yang, Q. Ren and Z. Bao, *Ind. Eng. Chem. Res.*, 2020, **59**, 7866-7874.

18 B. Liu and B. Smit, *J. Phys. Chem. C*, 2010, **114**, 8515-8522.

19 R. Zhong, Z. Xu, W. Bi, S. Han, X. Yu and R. Zou, *Inorg. Chim. Acta*, 2016, **443**, 299-303.

20 D. Lv, R. Shi, Y. Chen, Y. Chen, H. Wu, X. Zhou, H. Xi, Z. Li and Q. Xia, *Ind. Eng. Chem. Res.*, 2018, **57**, 12215-12224.

21 W. Liang, Z. Liu, J. Peng, X. Zhou, X. Wang and Z. Li, *Energ. Fuel.*, 2019, **33**, 493-502.

22 L. Zhang, K. Jiang, Y. Yang, Y. Cui, B. Chen and G. Qian, *J. Solid State Chem.*, 2017, **255**, 102-107.

23 R. Lin, R. Lin and B. Chen, *J. Solid State Chem.*, 2017, **252**, 138-141.

24 S. Xiang, Y. He, Z. Zhang, H. Wu, W. Zhou, R. Krishna and B. Chen, *Nat. Commun.*, 2012, **3**.

25 Z. Zhang, Q. Ding, J. Cui, X. Cui and H. Xing, *SCIENCE CHINA-MATERIALS*, 2021, **64**, 691-697.

26 N. Li, Z. Chang, H. Huang, R. Feng, W. He, M. Zhong, D.G. Madden, M.J. Zaworotko and X. Bu, *Small*, 2019, **15**.

27 B. Wang, A.P. Cote, H. Furukawa, M. O'Keeffe and O.M. Yaghi, *Nature*, 2008, **453**, 206-207.
28 Y. Xiong, Y. Fan, R. Yang, S. Chen, M. Pan, J. Jiang and C. Su, *Chem. Commun.*, 2014, **50**, 14631-14634.
29 P. Nugent, Y. Belmabkhout, S.D. Burd, A.J. Cairns, R. Luebke, K. Forrest, T. Pham, S. Ma, B. Space, L. Wojtas, M. Eddaoudi and M.J. Zaworotko, *Nature*, 2013, **495**, 80-84.
30 S. Xiang, Y. He, Z. Zhang, H. Wu, W. Zhou, R. Krishna and B. Chen, *Nat. Commun.*, 2012, **3**.
31 Z. Zhang, Q. Ding, S.B. Peh, D. Zhao, J. Cui, X. Cui and H. Xing, *Chem. Commun.*, 2020, **56**, 7726-7729.
32 H. Chen, L. Fan, X. Zhang and L. Ma, *ACS APPLIED NANO MATERIALS*, 2020, **3**, 2680-2686.
33 J. Dai, D. Xie, Y. Liu, Z. Zhang, Y. Yang, Q. Yang, Q. Ren and Z. Bao, *Ind. Eng. Chem. Res.*, 2020, **59**, 7866-7874.
34 D. Wu, C. Liu, J. Tian, F. Jiang, D. Yuan, Q. Chen and M. Hong, *Inorg. Chem.*, 2020, **59**, 13542-13550.
35 O.T. Qazvini, R. Babarao and S.G. Telfer, *Nat. Commun.*, 2021, **12**.
36 M. Jiang, B. Li, X. Cui, Q. Yang, Z. Bao, Y. Yang, H. Wu, W. Zhou, B. Chen and H. Xing, *ACS Appl. Mater. Inter.*, 2018, **10**, 16628-16635.
37 W. Liang, Z. Liu, J. Peng, X. Zhou, X. Wang and Z. Li, *Energ. Fuel.*, 2019, **33**, 493-502.
38 F. Yang, J. Wang, L. Liu, P. Zhang, W. Yu, Q. Deng, Z. Zeng and S. Deng, *ACS Sustain. Chem. Eng.*, 2018, **6**, 15550-15559.
39 D. Lv, J. Chen, K. Yang, H. Wu, Y. Chen, C. Duan, Y. Wu, J. Xiao, H. Xi, Z. Li and Q. Xia, *Chem. Eng. J.*, 2019, **375**.
40 H. Wen, C. Liao, L. Li, A. Alsalme, Z. Alothman, R. Krishna, H. Wu, W. Zhou, J. Hu and B. Chen, *J. Mater. Chem. A*, 2019, **7**, 3128-3134.
41 L. Yang, X. Cui, Y. Zhang, Q. Wang, Z. Zhang, X. Suo and H. Xing, *ACS Sustain. Chem. Eng.*, 2019, **7**, 3138.
42 B. Zhang, J. Yan and Z. Wang, *J. Phys. Chem. C*, 2018, **122**, 12831-12838.
43 Z.L. Ma, P.X. Liu, Z.Y. Liu, J.J. Wang, L.B. Li and L. Tian, *Inorg. Chem.*, 2021, **60**, 6550-6558.
44 Y. Ye, H. Zhang, L. Chen, S. Chen, Q. Lin, F. Wei, Z. Zhang and S. Xiang, *Inorg. Chem.*, 2019, **58**, 7754-7759.
45 S. Du, Y. Wu, X. Wang, Q. Xia, J. Xiao, X. Zhou and Z. Li, *AIChE J.*, 2020, **66**.
46 D. Lv, J. Chen, K. Yang, H. Wu, Y. Chen, C. Duan, Y. Wu, J. Xiao, H. Xi, Z. Li and Q. Xia, *Chem. Eng. J.*, 2019, **375**.
47 B. Zhang, J. Yan and Z. Wang, *J. Phys. Chem. C*, 2018, **122**, 12831-12838.